

1
2
3
4
5
6
7
8
9
10
11
12
13
14
15
16
17
18
19
20
21
22
23
24

MRS. MOLLY NAYLOR (Orcid ID : 0000-0001-6171-6748)

DR DANIEL E. MICHELE (Orcid ID : 0000-0003-4393-4551)

Received Date : 20-Feb-2020

Revised Date : 08-Jul-2020

Accepted Date : 08-Aug-2020

Article type : Original Article

Sarcolemma Wounding Activates Dynamin-Dependent Endocytosis in Striated Muscle

Joel R. McDade 1*#, Molly T. Naylor 1,2*, Daniel E Michele 1,2,3

1 Department of Molecular and Integrative Physiology, University of Michigan, Ann Arbor, MI 48103

2 Program in Cellular and Molecular Biology, University of Michigan, Ann Arbor, MI 48103

3 Department of Internal Medicine, Division of Cardiovascular Medicine, University of Michigan, Ann Arbor, MI 48103

*These authors contributed equally to this work

#Current Address: Oxford Genetics Limited, Cambridge, MA 02139

Corresponding author:

This is the author manuscript accepted for publication and has undergone full peer review but has not been through the copyediting, typesetting, pagination and proofreading process, which may lead to differences between this version and the [Version of Record](#). Please cite this article as [doi: 10.1111/FEBS.15556](https://doi.org/10.1111/FEBS.15556)

This article is protected by copyright. All rights reserved

25 Daniel E. Michele, PhD
26 University of Michigan
27 Department of Molecular and Integrative Physiology
28 207S NCRC, 2800 Plymouth Road
29 Ann Arbor, MI 48105
30 Email: dmichele@umich.edu

31

32 **Running Title:** Muscle wounding activates dynamin-dependent endocytosis

33 **Keywords:** skeletal muscle, membrane repair, membrane transport, endocytosis, dynamin, dysferlin

34 **Conflicts of Interest:** The authors have no conflicts to declare

35

36 **Abbreviations**

37 DMSO: Dimethyl Sulfoxide; Dysf-pHGFP: Dysferlin-pHLuorin; FBS: Fetal Bovine Serum; i.p.:
38 Intraperitoneal; MP: Multiphoton; NRK Cells: Normal Rat Kidney Epithelial Cells; PSS: Physiological Saline
39 Solution; WT: Wild-Type

40 **Abstract:**

41 Plasma membrane repair is an evolutionarily conserved mechanism by which cells can seal breaches in
42 the plasma membrane. Mutations in several proteins with putative roles in sarcolemma integrity,
43 membrane repair, and membrane transport result in several forms of muscle disease; however, the
44 mechanisms that are activated and responsible for sarcolemma resealing are not well understood. Using
45 the standard assays for membrane repair, which track the uptake of FM 1-43 dye into adult skeletal muscle
46 fibers following laser-induced sarcolemma disruption, we show that labeling of resting fibers by FM1-43
47 prior to membrane wounding and the induced FM1-43 dye uptake after sarcolemma wounding occurs *via*
48 dynamin-dependent endocytosis. Dysferlin-deficient muscle fibers show elevated dye uptake following
49 wounding, which is the basis for the assertion that membrane repair is defective in this model. Our data
50 show that dynamin inhibition mitigates the differences in FM1-43 dye uptake between dysferlin-null and
51 wild-type muscle fibers, suggesting that elevated wound-induced FM1-43 uptake in dysferlin-deficient
52 muscle may actually be due to enhanced dynamin-dependent endocytosis following wounding, though
53 dynamin inhibition had no effect on dysferlin trafficking after wounding. By monitoring calcium flux after
54 membrane wounding, we show that reversal of calcium precedes the sustained, slower increase of
55 dynamin-dependent FM1-43 uptake in WT fibers, and that dysferlin-deficient muscle fibers have
56 persistently increased calcium after wounding, consistent with its proposed role in resealing. These data
57 highlight a previously unappreciated role for dynamin-dependent endocytosis in wounded skeletal muscle
58 fibers and identify overactive dynamin-dependent endocytosis following sarcolemma wounding as a
59 potential mechanism or consequence of dysferlin deficiency.

60

61

62

63 **Introduction:**

64 Proper maintenance of the plasma membrane is critical in cardiac and skeletal muscle as
65 mutations that render the sarcolemma susceptible to membrane injury or disrupt membrane repair result
66 in muscle disease [1-3]. Mutations in several putative membrane transport proteins including dysferlin
67 [4], annexin [5], MG53 [6], synaptotagmin-VII [7] and PTRF/Cavin-1 [8] have been shown in mouse models
68 to result in muscle disease, potentially through reduced capacity to reseal the plasma membrane

69 following wounding [9]. This hypothesis is based largely on *in-vitro* laser-wounding experiments, which
70 demonstrate that mutant skeletal muscle cells take up excess extracellular FM-dyes compared to normal
71 cells following wounding [4, 6, 8]. One important caveat of these studies is that FM-dyes can also be taken
72 up by endocytosis [10], a possibility which has not been investigated in adult skeletal muscle fibers neither
73 at rest nor after injury. Early studies from non-muscle cells indicate that delivery and fusion of intracellular
74 vesicles with the plasma membrane is required for efficient wound repair [11-13]. On the basis of these
75 findings, most research on muscle membrane repair to date has focused on wound-induced exocytosis as
76 a means to reseal the sarcolemma. However, we have recently demonstrated that membrane wounding
77 induces endocytosis of at least one putative membrane repair protein, dysferlin, resulting in the formation
78 of large dysferlin-containing cytoplasmic vesicles [14], raising the intriguing possibility that endocytosis
79 may contribute to efficient membrane repair in adult skeletal muscle. In spite of this, there is very little
80 direct evidence that membrane wounding activates endocytic pathways in adult skeletal muscle, and
81 whether endocytosis contributes to membrane repair is not clear.

82 Dynamin is a large GTPase that facilitates endocytosis by forming oligomerized rings around
83 nascent vesicles leading to vesicle release. Mutations or deficiency of dynamin-2, a dynamin isoform
84 highly expressed in adult skeletal muscle, results in a centronuclear myopathy phenotype characterized
85 by internalized nuclei and t-tubule membrane and cytoskeletal disorganization by a largely unknown
86 mechanism [15, 16]. Dysferlin is mislocalized away from the sarcolemma in muscle from dynamin-2
87 heterozygous mutant mice, indicating that dynamin may regulate some aspect of dysferlin function [16],
88 but the relevance of this interaction to membrane repair has not been explored. Interestingly, dynamin-
89 dependent endocytosis contributes to membrane repair in NRK cells following perforin-induced injury by
90 removing toxin pores that assemble in the plasma membrane [17]. These data suggest that dynamin and
91 dynamin-dependent endocytosis may play a role in membrane repair, but whether dynamin-dependent
92 endocytosis is activated following sarcolemma wounding, and whether dysferlin and dynamin are
93 components of the same membrane repair pathway has not been explored.

94 We tested the overall hypothesis that dynamin-dependent endocytosis of dysferlin-containing
95 vesicles is critical for membrane repair following acute wounding in adult skeletal muscle fibers. We tested
96 this hypothesis by examining FM1-43 uptake into adult skeletal muscle fibers at rest and following laser-
97 induced wounding with or without pharmacological inhibition of dynamin-dependent endocytosis.
98 Surprisingly, basal and wound-induced FM1-43 uptake is severely reduced in skeletal muscle fibers treated
99 with a dynamin-inhibitor, indicating that wounding stimulates a large endocytic response that is measured

100 by FM1-43. We also use calcium flux following membrane wounding as an alternative approach to show
101 that the reversal of calcium precedes the slower and continued increase of FM1-43 uptake after
102 wounding, which suggests resealing and wound-induced increases in endocytosis may be distinct
103 temporal events in the membrane repair process. Together, these data have important implications for
104 future studies of membrane repair, give mechanistic insight into membrane repair in muscle, and highlight
105 the modulation of dynamin-activity as a potential therapeutic approach for muscle disease.

106 **Results:**

107 *FM1-43 uptake in resting adult skeletal muscle fibers requires dynamin activity.* Multiple membrane
108 transport proteins have been linked to muscle disease, including dynamin-2, and in some cell types,
109 endocytosis has been shown to play a critical role in plasma membrane repair [15, 17]. FM1-43 dye uptake
110 after laser wounding is a standard assay for membrane repair, but FM1-43 also has been used in other
111 cell types to monitor cellular endocytosis [10]. Little is known about the resting endocytic activity of adult
112 skeletal muscle fibers. The standard assay for membrane repair utilizes a preincubation of fibers in media
113 containing FM1-43 dye prior to laser-induced membrane wounding. Wild-type skeletal muscle fibers from
114 adult C57BL/6 mice were isolated and incubated with a solution containing 2.5 μ M FM1-43, which led to
115 a rapid increase in cellular fluorescence that reached maximal intensity at \sim 10 min post FM1-43 addition
116 (**Fig 1A**). To determine whether the prolonged increase in FM1-43 labeling was due to dye uptake *via*
117 endocytosis, resting adult skeletal muscle fibers were incubated with FM1-43 in the presence of DMSO \pm
118 dynasore, a potent inhibitor of dynamin-dependent endocytosis (outlined in **Fig 1B**). FM1-43 labeling in
119 resting adult skeletal muscle fibers was not affected by DMSO-treatment, (**Fig 1B top**, quantified **1C**) but
120 is almost completely abolished in the presence of dynasore (**Fig 1B middle**, quantified in **1C**). The inhibitory
121 effect of dynasore on FM1-43 labeling is reversible, as FM1-43 uptake commences upon removal of
122 dynasore from the extracellular solution (**Fig 1B bottom**, quantified **1D**). These data indicate that FM1-43
123 dye uptake *via* dynamin-dependent endocytosis is the major mechanism by which adult skeletal muscle
124 fibers become labeled with FM1-43 at rest.

125

126 *Wound-induced FM1-43 uptake is dynamin-dependent in adult skeletal muscle fibers.* Elevated wound-
127 induced FM1-43 fluorescence after membrane wounding has been assumed to occur by dye entry from
128 the extracellular buffer through nascent lesions and binding to intracellular lipids [18]. The accumulation
129 of dye fluorescence is commonly used as a gold standard assay to study membrane resealing and quantify

130 defective membrane repair [4, 6, 19]. However, previous studies have not definitively examined the
131 mechanism of how wound-induced dye uptake occurs, and whether this might be mediated by
132 endocytosis. Given that FM1-43 uptake in resting adult skeletal muscle fibers is highly dependent on
133 dynamin activity, we posited that wound-induced FM1-43 uptake may also be dynamin-dependent. To
134 test this, muscle fibers were isolated from adult C57BL/6 mice and "loaded" with FM1-43 for 10 minutes
135 to ensure equal and complete FM1-43 labeling prior to wounding. Once loaded, fibers were switched to
136 solution containing FM1-43 \pm dynasore, and subjected to laser-induced wounding (outlined in **Fig 2A**).
137 Consistent with our hypothesis, acute (~5 min) treatment with 80 μ M dynasore markedly reduced FM1-
138 43 uptake following wounding compared to DMSO treated control cells, and this effect was reversible
139 following removal of dynasore from the extracellular solution (**Fig 2B**, quantified **2C**). We independently
140 confirm these results using an even more potent inhibitor of dynamin, Dyngo4a, and show that Dyngo4a
141 also significantly decreases the uptake of FM1-43 after wounding (**Fig 2C**) [20]. These findings suggest that
142 membrane wounding elicits a considerable dynamin-dependent endocytic response that contributes to
143 FM1-43 uptake after wounding. We show that wound-induced FM1-43 uptake does not occur solely
144 through membrane lesions, but in fact the majority of wound-induced dye uptake occurs *via* dynamin-
145 dependent endocytosis in adult skeletal muscle fibers.

146 *FM1-43 uptake after membrane wounding is dependent upon extracellular dye.* To further exemplify that
147 the increase in FM1-43 fluorescence after wounding is caused by uptake of the extracellular dye in the
148 media, the plasma membrane of skeletal muscle fibers isolated from adult C57BL/6 mice was labeled with
149 FM1-43 for ~10min, and then all extracellular FM1-43 was removed, and the fibers were wounded in the
150 presence or absence of 80 μ M dynasore, (outlined in **Fig 3A**). We note that the washout of extracellular
151 FM1-43 removes a majority of the FM1-43 fluorescence that appears at the wound, and again, most of
152 the FM1-43 uptake in the presence of extracellular dye is inhibited by dynasore (**Fig 3B**, quantified **3C**).
153 These data suggest that FM1-43 is required in the extracellular media to produce wound-induced dye
154 uptake both by endocytic mechanisms (inhibited by dynasore) and through the membrane wound itself
155 (not inhibited by dynasore). Interestingly, however, there is a small area of FM1-43 fluorescence directly
156 at the wound that appears rapidly after wounding in the absence of extracellular FM1-43. This suggests that
157 lipids labeled by FM1-43 prior to wounding rapidly occupy the wounded area and can contribute to FM1-
158 43 fluorescence following a membrane wound, albeit to a smaller extent than dye uptake through
159 endocytosis and membrane lesions. Together this data suggests that dynamic movement of lipids through
160 endocytosis and other mechanisms, are significant contributors to wound induced FM1-43 uptake and

161 these mechanisms must be considered to fully appreciate the utility of FM1-43 for identifying contributing
162 mechanisms to membrane repair.

163 *Dynamin inhibition reduces wound-induced uptake of FM1-43 into wild-type and dysferlin-deficient*
164 *muscle fibers.* Dysferlin-deficiency has been shown to result in elevated uptake of FM1-43 after
165 membrane wounding, which is the basis for the assertion that dysferlin mutations result in defective
166 membrane repair [4]. Given that wound-induced FM1-43 uptake is dependent upon dynamin-activity in
167 wild-type muscle fibers, we posited that the elevated FM1-43 uptake observed in dysferlin-null skeletal
168 muscle fibers is due to over-activation of dynamin-dependent endocytosis following wounding. Neither
169 maximum FM1-43 labeling nor the rate of uptake were different between resting wild-type (A/WySnJ)
170 and dysferlin-null (A/J) muscle fibers, indicating that dysferlin-deficiency does not affect resting
171 dynamin-dependent FM1-43 uptake (**Fig 4A**). Consistent with previous reports, DMSO treated, wounded
172 A/J muscle fibers show increased uptake of FM1-43 after wounding. However, dynasore treatment
173 significantly reduced wound-induced FM1-43 uptake in both wild-type and dysferlin-null muscle fibers
174 and obscured any differences in FM1-43 uptake between the two genotypes (**Fig 4B**, quantified **4C**).
175 Consistent with our hypothesis, these data suggest that elevated wound-induced uptake of FM1-43 in
176 dysferlin-deficient muscle fibers may be actually due to elevated dynamin activity following wounding in
177 adult muscle fibers.

178 *Dynamin inhibition does not affect endocytosis of dysferlin following wounding in adult skeletal muscle*
179 *cells.* In order to determine whether dynamin and dysferlin are within the same membrane repair pathway
180 and if dynamin may regulate dysferlin function in some way, we tracked dysferlin trafficking following
181 wounding in the presence or absence of dynamin inhibition. We previously developed a dysferlin-pHluorin
182 muscle specific transgenic mouse (dysf-pHGFP) which allows for real-time tracking of dysferlin
183 endocytosis based on varying fluorescence intensity depending on the specific subcellular compartment
184 (outlined in **Fig 4D**) [21]. Consistent with our previous report, surface localized dysferlin-pHGFP molecules
185 adjacent to the lesion are rapidly recruited to the membrane wound (white arrow **Fig 4E**, quantified **4F**),
186 whereas remaining dysferlin-pHGFP molecules are rapidly quenched in response to wounding (red arrow
187 **Fig 4E**, quantified **4G**). Given the fact that dynamin-mediated endocytosis is activated in response to
188 wounding, we sought to examine whether dysferlin endocytosis is a dynamin-dependent pathway in adult
189 skeletal muscle fibers. To address this, real-time changes in dysferlin-pHGFP fluorescence intensity were
190 analyzed following wounding in adult dysf-pHGFP skeletal muscle fibers following treatment with DMSO
191 \pm 80 μ M dynasore. Our data indicate that treatment with dynasore does not affect recruitment of dysf-

192 pHGFP to membrane lesions (**Fig 4E**), or endocytosis following wounding (**Fig 4F**). Taken together, these
193 data indicate that while dynamin-dependent endocytosis is activated in response to wounding, dysferlin
194 trafficking to membrane wounds and dysferlin endocytosis after wounding is dynamin-independent.

195
196 *Calcium flux following membrane wounding indicates a rapid repair response as compared to FM1-43*
197 *uptake. Since we show that FM1-43 uptake after wounding is largely dependent upon wound-induced*
198 *endocytosis, we used calcium flux as an endocytosis-independent measure of membrane repair. Calcium*
199 *influx through membrane lesions is considered the proximal event following membrane disruption and*
200 *is thought to be required for activation of the membrane repair machinery [11, 22, 23]. Adult skeletal*
201 *muscle fibers isolated from adult C57BL/6 mice were incubated with 3 μ M Fluo-4, a fluorescent calcium*
202 *indicator, and intracellular calcium levels were measured following laser wounding. Membrane*
203 *wounding leads to a rapid increase in intracellular calcium concentration near the wound that peaks on*
204 *average around 40 sec post-wounding and decreases down to a steady state calcium concentration that*
205 *is higher than the pre-wounded level (**Fig 5A, B**). Shortly after wounding, calcium diffuses, increasing the*
206 *calcium concentration at sites distal to the wound that peaks and reverses near 60s post wound (**Fig 5C,***
207 ***D**). Fluo-4 fluorescence shows a clear peak and reversal which seems to suggest that shortly after*
208 *wounding, influx of extracellular calcium ions is restricted and calcium begins to be actively removed*
209 *from the cytoplasm.*

210 We also show that stimulating calcium release from the sarcoplasmic reticulum by treating
211 wounded myofibers with a bolus of caffeine (PSS+10mM Caffeine) increases cytoplasmic calcium above
212 calcium levels measured immediately after membrane wounding (**Fig. 5E**). These data indicate that the
213 reversal in Fluo-4 fluorescence is a direct result of decreased cytoplasmic calcium concentrations and
214 not artifact caused by dye leakage through the plasma membrane breach. These data suggest that Fluo-
215 4 under these conditions can capture the peak post-wound cytoplasmic calcium without saturating the
216 microscope detectors or binding capacity of the Fluo-4 indicator. We go on to show that cytoplasmic
217 calcium increases after wounding are dependent upon extracellular calcium flowing down its
218 electrochemical gradient as when extracellular calcium is removed and any trace amounts of calcium
219 chelated with 1mM EGTA, minimal changes in intracellular calcium concentrations are observed (**Fig 5F**).
220 Importantly, the kinetics of calcium reversal are rapid and in stark contrast to FM1-43 dye uptake, which
221 shows a bi-phasic response of an initial rapid increase followed by a gradual persistent increase in
222 fluorescence intensity over the course of several minutes post sarcolemma wounding (**Fig 5G**). Taken

223 together, these data confirm that measuring calcium concentrations provide a sensitive, robust assay for
224 the accurate indication of the point at which calcium influx slows and efflux mechanisms begin to
225 dominate, and can provide an important readout for when barrier function to the plasma membrane is
226 likely restored.

227 *Calcium influx after membrane wounding is largely dynamin-independent.* We show that FM1-43 uptake
228 after wounding is dependent upon dynamin activity and FM1-43 uptake shows markedly slow kinetics
229 compared to the estimates of wound-induced resealing as measured by calcium influx. To confirm that
230 calcium flux after wounding is not dependent upon dynamin activity, Fluo-4 loaded muscle fibers were
231 treated with 80 μ M dynasore or vehicle control (DMSO) and wounded. Following treatment and
232 wounding, muscle fibers show a rapid increase in calcium similar to vehicle control treated cells (**Fig 6A**,
233 quantified **6B**). There is a modest effect of dynasore treatment on the reversal of Fluo-4 fluorescence
234 that results in a slightly faster reversal in calcium toward baseline compared to vehicle control treated
235 cells (**Fig 5C**). These modest effects on cytoplasmic calcium after wounding suggest inhibition of
236 dynamin by dynasore has some effects on compartmentalization of calcium after wounding, but
237 importantly, the calcium influx immediately after membrane wounding is unaffected by dynasore
238 treatment. These data further support the conclusions that calcium influx and reversal is largely
239 dynamin-independent, and FM 1-43 uptake is largely dynamin-dependent and these two assays provide
240 complimentary insight into the distinct kinetic steps and mechanisms of membrane repair.

241 *Dysferlin-Deficient muscle fibers have increased calcium influx after wounding.* We showed that
242 dynasore treatment severely blunts the uptake of FM1-43 into wounded dysferlin-deficient muscle
243 fibers. We also show that dynasore treatment effectively removes any difference in FM1-43 uptake
244 between wild-type and dysferlin-deficient fibers. Therefore, we investigated whether calcium influx in
245 dysferlin-deficient muscle was increased compared to wild-type. Isolated muscle fibers from dysferlin-
246 deficient BLA/J mice and wild-type (C57BL/6) littermate controls were loaded with 3 μ M Fluo-4 and
247 laser-wounded. Immediately after wounding, calcium influx into dysferlin-deficient muscle is increased
248 compared to wild-type (**Fig 7A-D**). However, while the peak amount of calcium is increased in BLA/J
249 mice, calcium reverses similarly in both genotypes (solid line **Fig 7B, 7E**). Interestingly, while we noted
250 previously that calcium after wounding does not return to pre-wound levels in wild-type cells, this
251 persistent increase in calcium is exacerbated in dysferlin-deficient muscle fibers (**Fig 7F**).

252 **Discussion:**

253 Elevated uptake of extracellular dyes following laser-wounding has been noted in multiple models
254 of muscle disease; a phenotype that is commonly attributed to defective membrane repair following
255 membrane wounding. In fact, almost all experiments investigating the role of a given protein in membrane
256 repair have relied on measuring uptake of extracellular dyes following wounding. Importantly, FM1-43
257 uptake was traditionally used to measure endocytosis, but whether endocytosis is activated following
258 wounding in adult muscle fibers is unknown. In this study, we show that FM1-43 labeling in resting muscle
259 fibers is completely reduced in the presence of a dynamin inhibitor. Furthermore, wound-induced FM1-
260 43 uptake is significantly reduced when dynamin-dependent endocytosis is inhibited. These findings
261 strongly suggest that the FM1-43 uptake assay commonly used to assess repair capacity in skeletal muscle
262 fibers measures a combination of dye influx through membrane lesions and a massive endocytic response
263 to wounding and highlight a need for additional measures of membrane resealing in adult skeletal muscle.
264 We show that calcium influx after wounding occurs *via* a largely dynamin-independent mechanism, and
265 further highlight its utility in studying membrane repair by showing that dysferlin-deficiency results in
266 increased influx of calcium after wounding. These findings highlight a previously unappreciated role for
267 dynamin-dependent endocytosis in resting and wounded skeletal muscle and inform the membrane
268 resealing process in adult skeletal muscle.

269 There is still a significant lack of knowledge with regards to which transport pathways are
270 activated following wounding, and which membrane transport pathways contribute to membrane repair
271 in adult skeletal muscle. While evidence for lysosomal or organelle exocytosis in muscle membrane repair
272 exists [7, 24], the role of endocytosis in muscle membrane repair is largely unknown. The use of
273 extracellular, lipophilic FM-dyes (FM1-43 and FM4-64) to indirectly measure resealing capacity has
274 become the gold standard assay for membrane repair used as the primary method to identify putative
275 membrane repair proteins based on the general principle that flow of dye through lesions ("dye uptake")
276 should be greatest in cells with impaired membrane resealing. However, FM-dyes are classically used to
277 measure endocytosis following electrical stimulation or mechanical transection in neurons and the
278 possibility that a similar mechanism exists in adult skeletal muscle has never been examined [25]. Our
279 data in resting adult skeletal muscle fibers indicates that FM1-43 labeling is a gradual process that occurs
280 over several minutes, a finding that is more consistent with dye uptake as an active process rather than
281 simply passive labeling of the plasma membrane and t-tubules. Consistent with this interpretation, FM1-
282 43 labeling is almost completely abolished in the absence of dynamin activity, suggesting that FM1-43
283 labeling occurs *via* delivery of extracellular dye into undefined intracellular compartments through
284 dynamin-dependent endocytosis in adult skeletal muscle fibers.

285 A logical next step was to determine whether dynamin-mediated endocytosis is responsible for
286 any or all of the dye uptake that occurs following acute membrane wounding in adult skeletal muscle. Our
287 results suggest that the vast majority of wound-induced dye uptake is dependent upon dynamin activity,
288 which supports the overall conclusion that dynamin-dependent endocytosis is responsible for much of
289 the dye uptake that occurs following wounding. Dysferlin-deficient muscle as well as several other genetic
290 models of muscle disease show a characteristic elevation of wound-induced FM1-43 uptake, which is the
291 basis for the assertion that membrane resealing is impaired in this and other model systems [4, 26]. If
292 FM1-43 is measuring endocytosis, then it is possible that the “membrane repair deficiency” phenotype
293 commonly attributed to genetic models of muscle disease may actually be due to elevated wound-induced
294 endocytosis.

295 Direct comparison of FM1-43 uptake to calcium influx after wounding suggests membrane repair
296 is a much faster process than previously described by FM1-43 assays, and more consistent with previous
297 estimates of resealing kinetics [13]. The time course of FM1-43 appears to have both a fast component,
298 possibly due to entry through the lesion at the wound site and wound-induced endocytosis, and a slow
299 component, primarily due to wound-induced, dynamin-dependent endocytosis. These results indicate
300 that the two assays are measuring two separable entities, both of which could possibly play a role in
301 membrane repair. Wounding dramatically increases cytoplasmic calcium, followed by a quick reversal in
302 calcium concentrations measured by the fluorescent dyes loaded into cells. However, even several
303 minutes after wounding, calcium remains elevated globally and also compartmentalized in the cytoplasm
304 immediately adjacent to the wound. Prolonged elevation of calcium in the cytoplasm near and distal to
305 the wound could be a result of incomplete repair resulting in smaller, sustained calcium leak into the
306 cytoplasm. Indeed, while we interpret the reversal of calcium levels as an indicator of resealing, it could
307 also be interpreted as the time point where calcium efflux from the cytoplasm or *via* calcium reuptake
308 into organelles lacking Fluo-4, exceeds calcium influx through the wound. Previous work has suggested
309 that dysferlin may alter sarcoplasmic reticulum calcium handling [27] although Fluo-4 under the
310 experimental conditions here should load the sarcoplasmic reticulum as well, and thus altered SR function
311 may not explain the overall elevated calcium after sarcolemma wounding in dysferlin-deficient mice. The
312 localized high levels of calcium could be the result of calcium compartmentalization by organelles
313 proximal to the membrane wound. Recent work by Horn et. al. in differentiated myotubes showed that
314 calcium influx after laser wounding results in increased mitochondrial calcium that stimulates
315 mitochondrial ROS production, which interestingly, has a positive effect on membrane repair [28]. This is
316 consistent with the possibility that mitochondria or other organelles play a role in locally

317 compartmentalizing calcium after membrane wounding, but the contribution of individual organelle
318 compartments to calcium compartmentalization in adult fibers requires further experimentation. Finally,
319 calcium influx through membrane wounds, plays an important but complicated role in regulating many
320 aspects of muscle membrane repair. Calcium influx causes local muscle fiber contraction, and activates
321 the lipid binding properties of dysferlin[29] and annexins[30] which may play an important role in bringing
322 repair proteins and lipids to the membrane wound. Therefore, removing extracellular calcium in the
323 extracellular buffer actually increases FM1-43 uptake[31], despite calcium being important for activating
324 most forms of endocytosis in other cell types [32]. Prolonged excess intracellular calcium may also be
325 detrimental to fibers by disrupting excitation coupling, overactivating the mitochondrial permeability
326 transition pore and cell death, and/or downstream calcium-activated proteolysis, which may lead to
327 muscle fiber degeneration [33].

328 Whether wound-induced endocytosis contributes to membrane resealing or is a detrimental
329 consequence of sarcolemmal wounding is still unclear. One possibility is that membrane wounding
330 activates both an endocytic (*via* dynamin) and an exocytic response which both contribute to membrane
331 repair. In this case, mutant models could show if elevated dynamin-dependent endocytosis (FM1-43
332 uptake) is a compensatory response to facilitate membrane repair in the absence of other repair pathways
333 (such as wound-induced exocytosis) (**Fig 8A**). Dynamin-2 mutant mouse models, expressing mutations
334 associated with centranuclear myopathy, have a complicated phenotype due to its additional role in t-
335 tubule and triad biogenesis in muscle [34-36], but expression of dynamin-2 mutants does result in
336 elevated resting calcium in muscle [37]. Alternatively, wound-induced dynamin-dependent endocytosis
337 may be necessary to form an undefined population of membrane repair vesicles. In this scenario, elevated
338 dynamin-dependent endocytosis (FM1-43 uptake) in mutant models may indicate defective fusion of
339 nascent repair vesicles with the plasma membrane (**Fig 8B**). Indeed, accumulation of subsarcolemma
340 vesicles is a common observation in electron micrographs of muscle fibers from dysferlin deficient
341 muscular dystrophy patients and mice [4].

342 A balance of dynamin activity in muscle fibers is critical for muscle fiber health, as either genetic
343 loss or over-expression of dynamin-2 results in muscle disease [38]. Furthermore, dynamin expression is
344 elevated in a mouse model of myotubular myopathy and reducing dynamin levels restores muscle
345 structure and function [39]. Therefore, it is possible that elevated dynamin-activity following wounding
346 exacerbates muscle disease in membrane repair deficient skeletal muscles and reducing dynamin function
347 may be beneficial for muscle function. However, further work needs to be done to characterize dynamin

348 levels and potential post-translational modifications of dynamin that may give rise to enhanced dynamin-
349 dependent endocytosis following wounding in the various genetic models of membrane repair deficiency.
350 It is likely that dynamin acts in a separate pathway from that of dysferlin in membrane repair, as our data
351 indicates that inhibition of dynamin activity does not appear to affect dysferlin transport following
352 wounding (**Fig 4**). Thus, we propose the general model (shown in **Fig 8**) that a localized influx of calcium
353 through lesions activates dysferlin-mediated membrane repair, which feeds back to inhibit further calcium
354 influx and minimizes activation of dynamin-dependent endocytosis. In the absence of dysferlin, dysferlin-
355 mediated membrane repair is impaired, leading to an increased influx of calcium (**Fig 7**), over-activation
356 of dynamin-dependent endocytosis and activation of downstream, potentially pathological, pathways.

357 Our data reveal a potential role for dynamin in wound-induced endocytosis in membrane repair
358 and highlight modulation of dynamin levels or activity as a potential therapeutic approach for muscle
359 disease. Furthermore, this study demonstrates that several independent measurements of membrane
360 resealing capacity are needed and highlight that analysis of calcium dynamics in wounded cells may be a
361 useful tool for studying sarcolemma resealing. Future work will focus on assessing inhibition of
362 overactivated dynamin-activity as a therapeutic approach in dysferlin-deficiency.

363

364 **Materials and Methods:**

365 Animals: Wild-type (C57BL/6 or A/WySnJ) and dysferlin deficient (A/J) mice were purchased from Jackson
366 Laboratories, Bar Harbor, ME. Dysferlin-deficient BLA/J mice harbor the same mutation as A/J mice on a
367 C57BL/6 background and were a gift from The Jain Foundation Inc. [40]. Dysferlin-pHluorin (Dysf-pHGFP)
368 transgenic mice were generated as previously described [21]. All procedures with animals were approved
369 by the Institutional Animal Care and Use Committee at the University of Michigan.

370

371 Muscle fiber isolation and imaging setup: Muscle fibers were isolated and imaged as previously
372 described [11]. Briefly, flexor digitorum brevis muscles were isolated from the hind-paws of
373 anaesthetized (i.p. injection of 15 μ l/gram of 2.5% Avertin solution) wild-type, dysferlin-deficient or Dysf-
374 pHGFP transgenic mice and incubated for 4 hours at 37°C in an MEM solution containing 0.2%
375 collagenase. Muscle fibers were triturated with glass pipettes of decreasing radius to liberate individual
376 muscle fibers. Muscle fibers were plated on 35-mm glass bottom dishes and incubated at 37°C in MEM +
377 10% FBS until used. All live cell imaging was carried out on a Leica SP8 confocal microscope equipped

378 with a temperature controlled chamber. Cells were imaged through a 63x oil objective using an argon
379 laser (excitation wavelength of 488nm) and an HyD detector set from either 498-525nm (GFP, Fluo-4), or
380 580-620nm (FM1-43). Wounding was carried out by imaging a 2x2 μ m ROI at the sarcolemma using an
381 MP laser at ~70% power. In general, images were acquired every 1.3 seconds for ~3min. Photobleach
382 controls were carried out when necessary to ensure minimal dye uptake or GFP bleaching as a result of
383 imaging.

384

385 FM1-43 uptake assay: For analysis of FM1-43 uptake in resting muscle fibers, cells were imaged in residual
386 physiological saline solution (PSS: 15mM Hepes, 145mM NaCl, 5.6mM KCl, 2.2mM CaCl₂, 0.5mM MgCl₂,
387 and 5.6mM dextrose) to obtain a "baseline" recording of fluorescence intensity. Media was then changed
388 to PSS containing 2.5 μ M FM1-43 (Invitrogen: T3163) and cells were imaged using the FM1-43 imaging set-
389 up described above at a frame rate of 1/30 sec for a total of 15 min. To examine the effect of dynasore on
390 resting FM1-43 uptake, muscle cells were first incubated in PSS containing DMSO \pm 80 μ M dynasore (no
391 FM1-43) for 5-40 min and subsequently switched to the appropriate dye containing solution (\pm dynasore).
392 Laser-wounding assays were performed similar to previously published protocols [4, 21]. Briefly, cells
393 were pre-incubated for 10min in physiological saline containing 2.5 μ M FM1-43 to ensure complete
394 labeling of all exposed membrane compartments. Fibers were then subjected to laser-induced wounding
395 as described above. The multiphoton laser was calibrated prior to every experiment and was used at a
396 fixed intensity for the duration of each experiment to ensure production of equivalent wounds across all
397 cells. To examine the effect of dynasore on wound-induced FM1-43 uptake, cells were "loaded" for 10min
398 with FM1-43 to ensure equal labeling prior to wounding, incubated for 5 min in PSS + FM1-43 \pm dynasore,
399 and subjected to laser-induced wounding.

400

401 Calcium influx assays: Isolated fibers were incubated with 3 μ M Fluo-4-AM (Invitrogen: F-14201) diluted
402 in MEM+10%FBS for 60min at 37°C [41]. Cells were washed once with MEM+10%FBS and incubated for
403 10min at 37°C to allow cleavage by esterases and reduce dye leakage. Prior to imaging, media was
404 changed to PSS and fibers subjected to laser wounding as described above. Fluorescence intensity at the
405 wound was quantified by a 10x10 μ m ROI centered at the wound and distal fluorescence intensity was
406 quantified using a 10x10 μ m ROI placed on the membrane opposite the wound. Fluorescence intensity is

407 plotted as $\Delta F/F_0 ((F_t - F_0)/F_0)$ and the time to reversal in Fluo-4 experiments was estimated as the
408 inflection point on the first derivative graph of this time course.

409

410

411 **Author contributions:** J.R.M. and M.T.N. performed the research and analyzed the data. J.R.M., M.T.N.,
412 and D.E.M. designed the research and wrote the paper.

413

414 **Acknowledgements:** The authors thank Ashley Cuttitta and Patrick Thrasher for technical support and
415 The University of Michigan Microscopy and Image Analysis Laboratory for expert microscopy support.

416 This work has been supported by the American Heart Association (#12PRE12050130) to J.R.M., the NIH

417 Cellular and Molecular Biology Training Grant T-32-GM007315 and NIH Cardiovascular Research and

418 Entrepreneurship Training Grant T32-HL125242 to M.T.N., and research support was from NIH NIAMS

419 AR066213 and AR068428 to D.E.M.

420

421

Author Manuscript

423 **References:**

- 424 1. Allen, D. G., Whitehead, N. P. & Froehner, S. C. (2016) Absence of Dystrophin Disrupts Skeletal Muscle
425 Signaling: Roles of Ca²⁺, Reactive Oxygen Species, and Nitric Oxide in the Development of Muscular
426 Dystrophy, *Physiological reviews*. **96**, 253-305.
- 427 2. Claflin, D. R. & Brooks, S. V. (2008) Direct observation of failing fibers in muscles of dystrophic mice
428 provides mechanistic insight into muscular dystrophy, *American Journal of Physiology - Cell Physiology*.
429 **294**, C651-C658.
- 430 3. Bashir, R., Britton, S., Strachan, T., Keers, S., Vafiadaki, E., Lako, M., Richard, I., Marchand, S., Bourg, N.,
431 Argov, Z., Sadeh, M., Mahjneh, I., Marconi, G., Passos-Bueno, M. R., Moreira, E. d. S., Zatz, M., Beckmann,
432 J. S. & Bushby, K. (1998) A gene related to *Caenorhabditis elegans* spermatogenesis factor *fer-1* is mutated
433 in limb-girdle muscular dystrophy type 2B, *Nature Genetics*. **20**, 37-42.
- 434 4. Bansal, D., Miyake, K., Vogel, S. S., Groh, S., Chen, C.-C., Williamson, R., McNeil, P. L. & Campbell, K. P.
435 (2003) Defective membrane repair in dysferlin-deficient muscular dystrophy, *Nature*. **423**, 168-172.
- 436 5. Lennon, N. J., Kho, A., Bacskai, B. J., Perlmutter, S. L., Hyman, B. T. & Brown, R. H. (2003) Dysferlin
437 Interacts with Annexins A1 and A2 and Mediates Sarcolemmal Wound-healing, *Journal of Biological*
438 *Chemistry*. **278**, 50466-50473.
- 439 6. Cai, C., Masumiya, H., Weisleder, N., Matsuda, N., Nishi, M., Hwang, M., Ko, J.-K., Lin, P., Thornton, A.,
440 Zhao, X., Pan, Z., Komazaki, S., Brotto, M., Takeshima, H. & Ma, J. (2009) MG53 nucleates assembly of cell
441 membrane repair machinery, *Nat Cell Biol*. **11**, 56-64.
- 442 7. Chakrabarti, S., Kobayashi, K. S., Flavell, R. A., Marks, C. B., Miyake, K., Liston, D. R., Fowler, K. T.,
443 Gorelick, F. S. & Andrews, N. W. (2003) Impaired membrane resealing and autoimmune myositis in
444 synaptotagmin VII-deficient mice, *J Cell Biol*. **162**, 543-549.
- 445 8. Zhu, H., Lin, P., De, G., Choi, K.-h., Takeshima, H., Weisleder, N. & Ma, J. (2011) Polymerase
446 Transcriptase Release Factor (PTRF) Anchors MG53 Protein to Cell Injury Site for Initiation of Membrane
447 Repair, *Journal of Biological Chemistry*. **286**, 12820-12824.
- 448 9. Demonbreun, A. R. & McNally, E. M. (2016) Plasma Membrane Repair in Health and Disease, *Curr Top*
449 *Membr*. **77**, 67-96.
- 450 10. Ryan, T. A., Reuter, H. & Smith, S. J. (1997) Optical detection of a quantal presynaptic membrane
451 turnover, *Nature*. **388**, 478-82.
- 452 11. Bi, G. Q., Alderton, J. M. & Steinhardt, R. A. (1995) Calcium-regulated exocytosis is required for cell
453 membrane resealing, *J Cell Biol*. **131**, 1747-1758.

- 454 12. Bi, G.-Q., Morris, R. L., Liao, G., Alderton, J. M., Scholey, J. M. & Steinhardt, R. A. (1997) Kinesin- and
455 Myosin-driven Steps of Vesicle Recruitment for Ca²⁺-regulated Exocytosis, *J Cell Biol.* **138**, 999-1008.
- 456 13. Steinhardt, R., Bi, G. & Alderton, J. (1994) Cell membrane resealing by a vesicular mechanism similar
457 to neurotransmitter release, *Science.* **263**, 390-393.
- 458 14. McDade, J. R. & Michele, D. E. (2014) Membrane damage-induced vesicle-vesicle fusion of dysferlin-
459 containing vesicles in muscle cells requires microtubules and kinesin, *Hum Mol Genet.* **23**, 1677-86.
- 460 15. Bitoun, M., Maugenre, S., Jeannet, P.-Y., Lacene, E., Ferrer, X., Laforet, P., Martin, J.-J., Laporte, J.,
461 Lochmuller, H., Beggs, A. H., Fardeau, M., Eymard, B., Romero, N. B. & Guicheney, P. (2005) Mutations in
462 dynamin 2 cause dominant centronuclear myopathy, *Nat Genet.* **37**, 1207-1209.
- 463 16. Durieux, A.-C., Vignaud, A., Prudhon, B., Viou, M. T., Beuvin, M., Vassilopoulos, S., Fraysse, B., Ferry,
464 A., Lainé, J., Romero, N. B., Guicheney, P. & Bitoun, M. (2010) A centronuclear myopathy-dynamin 2
465 mutation impairs skeletal muscle structure and function in mice, *Human Molecular Genetics.* **19**, 4820-
466 4836.
- 467 17. Thiery, J., Keefe, D., Saffarian, S., Martinvalet, D., Walch, M., Boucrot, E., Kirchhausen, T. & Lieberman,
468 J. (2010) *Perforin activates clathrin- and dynamin-dependent endocytosis, which is required for plasma*
469 *membrane repair and delivery of granzyme B for granzyme-mediated apoptosis.*
- 470 18. McNeil, P. L., Miyake, K. & Vogel, S. S. (2003) The endomembrane requirement for cell surface repair,
471 *Proceedings of the National Academy of Sciences.* **100**, 4592-4597.
- 472 19. Cai, C., Weisleder, N., Ko, J.-K., Komazaki, S., Sunada, Y., Nishi, M., Takeshima, H. & Ma, J. (2009)
473 Membrane Repair Defects in Muscular Dystrophy Are Linked to Altered Interaction between MG53,
474 Caveolin-3, and Dysferlin, *Journal of Biological Chemistry.* **284**, 15894-15902.
- 475 20. McCluskey, A., Daniel, J. A., Hadzic, G., Chau, N., Clayton, E. L., Mariana, A., Whiting, A., Gorgani, N.
476 N., Lloyd, J., Quan, A., Moshkanbaryans, L., Krishnan, S., Perera, S., Chircop, M., von Kleist, L., McGeachie,
477 A. B., Howes, M. T., Parton, R. G., Campbell, M., Sakoff, J. A., Wang, X., Sun, J. Y., Robertson, M. J., Deane,
478 F. M., Nguyen, T. H., Meunier, F. A., Cousin, M. A. & Robinson, P. J. (2013) Building a better dynasore: the
479 dyngo compounds potently inhibit dynamin and endocytosis, *Traffic.* **14**, 1272-89.
- 480 21. McDade, J. R., Archambeau, A. & Michele, D. E. (2014) Rapid actin-cytoskeleton-dependent
481 recruitment of plasma membrane-derived dysferlin at wounds is critical for muscle membrane repair, *The*
482 *FASEB Journal.* **28**, 3660-3670.
- 483 22. Covian-Nares, J. F., Koushik, S. V., Puhl, H. L., III & Vogel, S. S. (2010) Membrane wounding triggers
484 ATP release and dysferlin-mediated intercellular calcium signaling, *J Cell Sci.* **123**, 1884-1893.

- 485 23. Mellgren, R. L., Miyake, K., Kramerova, I., Spencer, M. J., Bourg, N., Bartoli, M., Richard, I., Greer, P.
486 A. & McNeil, P. L. (2009) Calcium-dependent plasma membrane repair requires m- or [mu]-calpain, but
487 not calpain-3, the proteasome, or caspases, *Biochimica et Biophysica Acta (BBA) - Molecular Cell Research*.
488 **1793**, 1886-1893.
- 489 24. Cheng, X., Zhang, X., Gao, Q., Ali Samie, M., Azar, M., Tsang, W. L., Dong, L., Sahoo, N., Li, X., Zhuo, Y.,
490 Garrity, A. G., Wang, X., Ferrer, M., Dowling, J., Xu, L., Han, R. & Xu, H. (2014) The intracellular Ca²⁺ channel
491 MCOLN1 is required for sarcolemma repair to prevent muscular dystrophy, *Nat Med*. **20**, 1187-1192.
- 492 25. Betz, W. J., Bewick, G. S. & Ridge, R. M. A. P. (1992) Intracellular Movements of Fluorescently Labeled
493 Synaptic Vesicles in Frog Motor-Nerve Terminals during Nerve-Stimulation, *Neuron*. **9**, 805-813.
- 494 26. Han, R., Bansal, D., Miyake, K., Muniz, V. P., Weiss, R. M., McNeil, P. L. & Campbell, K. P. (2007)
495 Dysferlin-mediated membrane repair protects the heart from stress-induced left ventricular injury, *The*
496 *Journal of Clinical Investigation*. **117**, 1805-1813.
- 497 27. Kerr, J. P., Ziman, A. P., Mueller, A. L., Muriel, J. M., Kleinhans-Welte, E., Gumerson, J. D., Vogel, S. S.,
498 Ward, C. W., Roche, J. A. & Bloch, R. J. (2013) Dysferlin stabilizes stress-induced Ca²⁺ signaling in the
499 transverse tubule membrane, *Proceedings of the National Academy of Sciences*. **110**, 20831-20836.
- 500 28. Horn, A., Van der Meulen, J. H., Defour, A., Hogarth, M., Sreetama, S. C., Reed, A., Scheffer, L., Chandel,
501 N. S. & Jaiswal, J. K. (2017) Mitochondrial redox signaling enables repair of injured skeletal muscle cells,
502 *Science Signaling*. **10**, eaaj1978.
- 503 29. Abdullah, N., Padmanarayana, M., Marty, N. J. & Johnson, C. P. (2014) Quantitation of the calcium
504 and membrane binding properties of the C2 domains of dysferlin, *Biophys J*. **106**, 382-9.
- 505 30. Gerke, V., Creutz, C. E. & Moss, S. E. (2005) Annexins: linking Ca²⁺ signalling to membrane dynamics,
506 *Nat Rev Mol Cell Biol*. **6**, 449-61.
- 507 31. Bansal, D., Miyake, K., Vogel, S. S., Groh, S., Chen, C. C., Williamson, R., McNeil, P. L. & Campbell, K. P.
508 (2003) Defective membrane repair in dysferlin-deficient muscular dystrophy, *Nature*. **423**, 168-72.
- 509 32. Wu, X.-S., McNeil, B. D., Xu, J., Fan, J., Xue, L., Melicoff, E., Adachi, R., Bai, L. & Wu, L.-G. (2009) Ca²⁺
510 and calmodulin initiate all forms of endocytosis during depolarization at a nerve terminal, *Nature*
511 *Neuroscience*. **12**, 1003-1010.
- 512 33. Burr, A. R. & Molkentin, J. D. (2015) Genetic evidence in the mouse solidifies the calcium hypothesis
513 of myofiber death in muscular dystrophy, *Cell Death & Differentiation*. **22**, 1402-1412.
- 514 34. Chin, Y. H., Lee, A., Kan, H. W., Laiman, J., Chuang, M. C., Hsieh, S. T. & Liu, Y. W. (2015) Dynamin-2
515 mutations associated with centronuclear myopathy are hypermorphic and lead to T-tubule
516 fragmentation, *Hum Mol Genet*. **24**, 5542-54.

- 517 35. Cowling, B. S., Toussaint, A., Amoasii, L., Koebel, P., Ferry, A., Davignon, L., Nishino, I., Mandel, J. L. &
518 Laporte, J. (2011) Increased expression of wild-type or a centronuclear myopathy mutant of dynamin 2 in
519 skeletal muscle of adult mice leads to structural defects and muscle weakness, *Am J Pathol.* **178**, 2224-35.
- 520 36. Gibbs, E. M., Davidson, A. E., Telfer, W. R., Feldman, E. L. & Dowling, J. J. (2014) The myopathy-causing
521 mutation DNM2-S619L leads to defective tubulation in vitro and in developing zebrafish, *Dis Model Mech.*
522 **7**, 157-61.
- 523 37. Fraysse, B., Guicheney, P. & Bitoun, M. (2016) Calcium homeostasis alterations in a mouse model of
524 the Dynamin 2-related centronuclear myopathy, *Biol Open.* **5**, 1691-1696.
- 525 38. Cowling, B. S., Toussaint, A., Amoasii, L., Koebel, P., Ferry, A., Davignon, L., Nishino, I., Mandel, J.-L. &
526 Laporte, J. Increased Expression of Wild-Type or a Centronuclear Myopathy Mutant of Dynamin 2 in
527 Skeletal Muscle of Adult Mice Leads to Structural Defects and Muscle Weakness, *Am J Pathol.* **178**, 2224-
528 2235.
- 529 39. Cowling, B. S., Chevremont, T., Prokic, I., Kretz, C., Ferry, A., Coirault, C., Koutsopoulos, O., Laugel, V.,
530 Romero, N. B. & Laporte, J. (2014) Reducing dynamin 2 expression rescues X-linked centronuclear
531 myopathy, *The Journal of Clinical Investigation.* **124**, 1350-1363.
- 532 40. Lostal, W., Bartoli, M., Bourg, N., Roudaut, C., Bentaïb, A., Miyake, K., Guerchet, N., Fougèrouse, F.,
533 McNeil, P. & Richard, I. (2010) Efficient recovery of dysferlin deficiency by dual adeno-associated vector-
534 mediated gene transfer, *Human Molecular Genetics.* **19**, 1897-1907.
- 535 41. Park, K. H., Weisleder, N., Zhou, J. S., Gumpfer, K., Zhou, X. Y., Duann, P., Ma, J. J. & Lin, P. H. (2014)
536 Assessment of Calcium Sparks in Intact Skeletal Muscle Fibers, *Jove-J Vis Exp.*

537

538 **Figure Legends:**

539 **Figure 1. Resting adult skeletal muscle fibers take up FM1-43 via a dynamin-dependent mechanism.**

540 **FM1-43 labeling occurs over several minutes in adult skeletal muscle fibers.** FM1-43 uptake was

541 assessed in untreated, resting adult C57BL/6 skeletal muscle fibers (**A**) and in resting adult skeletal

542 muscle fibers following pre-treatment with DMSO or dynamin inhibitor dynasore (**B**). Untreated and

543 DMSO treated fibers take up extracellular FM1-43 with maximal labeling occurring within 10min (**A** and

544 **B** top, respectively, quantified in **C**). Pre-treatment with 80µM dynasore completely inhibits FM1-43

545 uptake in resting skeletal muscle fibers (**B**, middle, quantified in **C**). Dynasore-treated muscle fibers take

546 up FM1-43 following removal of dynasore from the extracellular solution (**C** bottom, quantified **D**). The

547 red scale bar indicates 50µm. Statistical comparisons were performed using an unpaired, two-tailed

548 Student's t-test. Statistical significance ($p < 0.05$) between DMSO and Dynasore is denoted by (*) for each
549 timepoint under the horizontal bar. Error bars represent the standard deviation of the mean. Data is
550 summarized from three independent loading plates.

551

552 **Figure 2. Wound-induced FM1-43 uptake is dynamin dependent in adult skeletal muscle fibers.**

553 C57BL/6 muscle fibers were loaded with FM1-43 normally, treated with DMSO +/- 80 μ M dynasore and
554 subjected to laser-induced wounding (**A**). Dynasore treatment (middle **B**, magenta squares in **C**) results
555 in significantly reduced wound-induced FM1-43 uptake compared to DMSO treated control cells (top **B**,
556 black circles in **C**). FM1-43 uptake in dynasore-washout cells was not significantly different than DMSO
557 treated controls, indicating a reversible effect of dynasore treatment on wound-induced FM1-43 uptake
558 in skeletal muscle cells (bottom **B**, teal triangles **C**). These results were independently confirmed using
559 the same experimental setup (**A**) with an additional dynamin inhibitor, Dyngo4a, again showing that
560 dynamin inhibition results in significantly reduced wound-induced FM1-43 uptake compared to DMSO
561 controls, which is reversible upon Dyngo4A washout (**C**). Statistical comparisons were performed using a
562 Two-Way ANOVA followed by posthoc Student's t-tests. Statistical significance ($p < 0.05$) between DMSO
563 and Dynasore/Dyngo4A is denoted by (*) and between Dynasore/Dyngo4a and Washout by (#) for each
564 timepoint under horizontal bar. **N.S.** designates no statistical difference ($p > 0.05$) between DMSO and
565 Washout conditions in both **C** and **D**. Error bars represent the standard deviation of the mean. One
566 representative experiment of three independent replicates (**B-C**) or two independent replicates (**D**) is
567 shown.

568

569 **Figure 3. FM1-43 uptake after wounding is dependent upon extracellular FM1-43.** Isolated skeletal

570 muscle fibers from adult C57BL/6 mice were loaded with 2.5 μ M FM1-43 for ~10min and wounded in the
571 presence or absence of Dynasore (**A**). Washout conditions were removed of extracellular FM1-43 and
572 cells then wounded in the presence or absence of dynasore. Representative images of all conditions
573 show that FM1-43 washout severely decreases FM1-43 fluorescence after wounding, however there is a
574 rapid accumulation of dye at the wound that is uninhibited by Dynasore treatment (**B**, quantified, **C**).
575 Statistical comparisons were performed using an unpaired, two-tailed Student's t-test (**A**) or Two-Way
576 ANOVA followed by posthoc Student's t-tests (**C**). The threshold for statistical significance was not met
577 in **A** ($p > 0.05$), but statistical significance ($p < 0.05$) between FM1-43+DMSO and all other traces is
578 denoted by (*) for each timepoint under the horizontal bar. Error bars represent the standard deviation
579 of the mean. One representative experiment of two independent replicates is shown.

580

581 **Figure 4. Dynamin is required for increased wound-induced uptake of FM1-43 in dysferlin-null muscle**
582 **fibers.** Basal FM1-43 uptake is unchanged in dysferlin-null A/J muscle fibers compared to A/WySnJ wild-
583 type controls(**A**). DMSO-treated, dysferlin null muscle fibers (representative images **B**, magenta triangles
584 in **C**) take up more FM1-43 dye following wounding than wild-type controls (representative images **B**,
585 black circles in **C**). Dynasore treatment significantly reduces wound-induced FM1-43 uptake in wild-type
586 and dysferlin-null muscle fibers (representative images **B**, open black circles and open magenta triangles
587 in **C**, respectively). Statistical comparisons were performed using Student's t-tests. Statistical significance
588 ($p < 0.05$) between A/J DMSO and A/J Dyna is denoted by (*) and between A/WySnJ DMSO and A/WySnJ
589 Dyna by (#) and between A/WySnJ DMSO and A/J DMSO by (^) for each timepoint under horizontal bar.
590 **N.S.** designates no statistical difference ($p > 0.05$) between A/WySnJ Dyna and A/J Dyna. The dysf-pHGFP
591 TG reporter mouse provides a real-time assessment of dysferlin localization in adult skeletal muscle
592 fibers (**D**). Recruitment of dysferlin to lesions (white arrowhead **E**, quantified **F**) and endocytosis of
593 dysferlin following wounding (red arrowhead **E**, quantified **G**) are unchanged in dynasore-treated cells,
594 indicating that dynamin activity is not required for dysferlin transport following wounding. Statistical
595 comparisons were made using an unpaired, two-tailed Student's t-tests and did not meet the threshold
596 of significance ($p > 0.05$). Error bars represent the standard deviation of the mean. One representative
597 experiment of three independent replicates (**A**), one independent replicate (**B-C**), and two independent
598 replicates (**D-G**) is shown.

599

600 **Figure 5. Calcium influx into the cell as measured by Fluo-4 relative fluorescence shows membrane**
601 **repair is a much faster process than as previously indicated by FM1-43 wounding studies.** Isolated
602 wild-type C57BL/6 muscle fibers were loaded with $3\mu\text{M}$ Fluo-4 for 1hr and then wounded with a high
603 powered laser, representative images shown (top **A**). Calcium increases at the wound site were
604 quantified, described by the white box in **B**, which showed that wounding causes a rapid increase in
605 calcium at the wound site (one representative trace shown **B**, summary data from one representative
606 experiment **C**). Calcium increases at the wound are followed by an increase in cytoplasmic calcium at
607 sites distal to the wound (red box in **B**, and magenta open circles **C**). Calcium at the wound peaks and
608 reverses at the wound at approximately 40s post wound (solid line **B**, summary data in **D**), but
609 cytoplasmic calcium reversal is significantly delayed to approximately 60s (**D**) A bolus of 10mM caffeine
610 to wounded fibers, one representative trace shown, stimulates calcium release from the SR that exceeds
611 peak calcium after wounding (**E**). Removing calcium from extracellular media and chelating any trace

612 calcium with 1mM EGTA prevents the increase in cytosolic calcium following wounding (representative
613 images **A** bottom, quantified **F**). While calcium flux reverses within the first minute following wounding,
614 the concentration of FM1-43 rises in the cell for more than 2 minutes, and then continues to increase at
615 a constant rate even after 2 minutes (**G**). Statistical comparisons were performed using an unpaired, two-
616 tailed Student's t-test. Statistical significance ($p < 0.05$) is denoted by (*). Error bars represent the
617 standard error of the mean. One representative experiment of three independent replicates is shown.

618 **Figure 6. Dynamin inhibition does not affect calcium influx after membrane wounding.** Isolated wild-
619 type C57BL/6 muscle fibers were loaded with 3 μ M Fluo-4 for 1hr and treated either with a vehicle
620 (DMSO, top panel) or 80 μ M Dynasore (bottom panel) prior to wounding shows calcium influx after
621 wounding is uninhibited by Dynasore treatment (representative images **A**, quantified **B**). Quantification
622 of the time at which the calcium signal peaks and reverses across 6 independent replicates shows
623 Dynasore treated cells have a faster time to peak calcium compared to vehicle control (**C**). Statistical
624 comparisons were performed using a Two-Way ANOVA followed by posthoc Student's t-tests. Statistical
625 significance ($p < 0.05$) between Dynasore and both PSS and Washout is denoted by (*). Error bars
626 represent the standard error of the mean.

627
628 **Figure 7. Dysferlin-deficiency muscle fibers have persistently elevated calcium after membrane**
629 **wounding.** Isolated muscle fibers from dysferlin-deficient BLA/J mice and wild-type littermate controls
630 (C57BL/6) were loaded with 3 μ M Fluo-4 for 1hr and wounded with a high-powered laser (representative
631 images **A**). Calcium concentrations after wounding are increased in dysferlin-deficient fibers (individual
632 traces **B**, summary of one experiment **C**), Peak calcium was normalized to WT peak calcium and pooled
633 among three independent replicates shown that peak calcium influx is increased in dysferlin-deficient
634 cells (**D**), but the time to calcium reversal is similar in WT and dysferlin-deficient cells (solid line **D**,
635 summary **E**). The steady state calcium at the end of imaging for three independent replicates was
636 normalized to WT steady state calcium, which is also greater in dysferlin deficient cells (**F**). Statistical
637 comparisons were performed using an unpaired, two-tailed Student's t-test. Statistical significance
638 ($p < 0.05$) between WT and BLA/J is denoted by (*). Error bars represent the standard error of the mean.

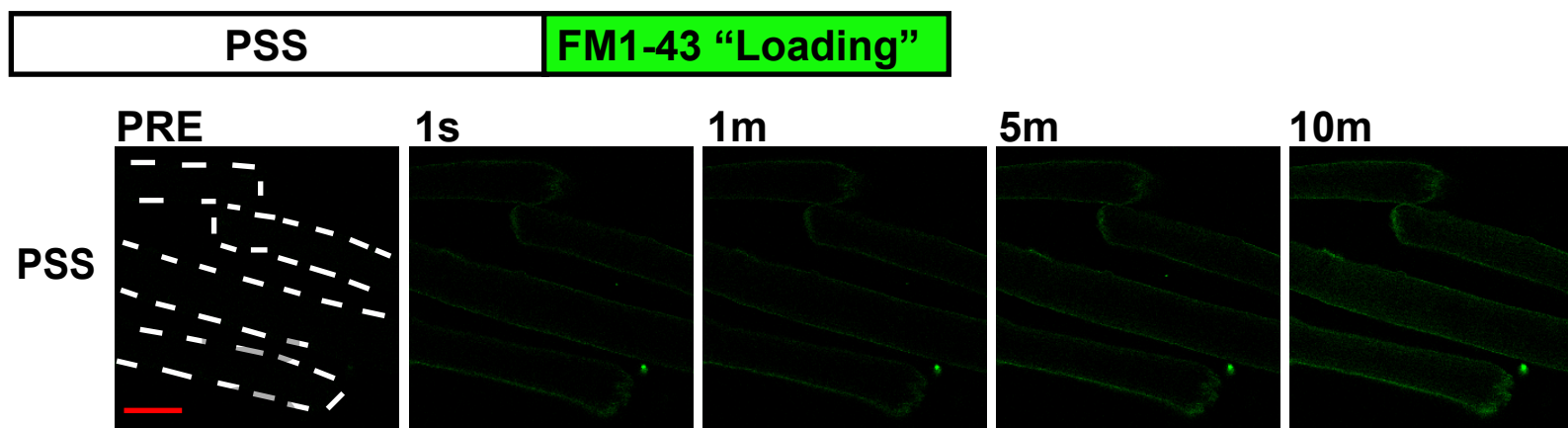
639
640

641 **Figure 8. General model of dynamin-mediated endocytosis and dysferlin-mediated membrane repair**
642 **in skeletal muscle.** In normal muscle, sarcolemma wounding leads to localized calcium influx and
643 activation of dysferlin-mediated membrane repair, preventing over-activation of dynamin-mediated
644 endocytosis (**A**). In dysferlin-deficient muscle wherein dysferlin-mediated repair is impaired, prolonged
645 calcium influx through unsealed lesions leads to increased activation of dynamin-dependent endocytosis
646 which may compensate for impaired dysferlin-MMR or contribute to disease pathology (**B**).

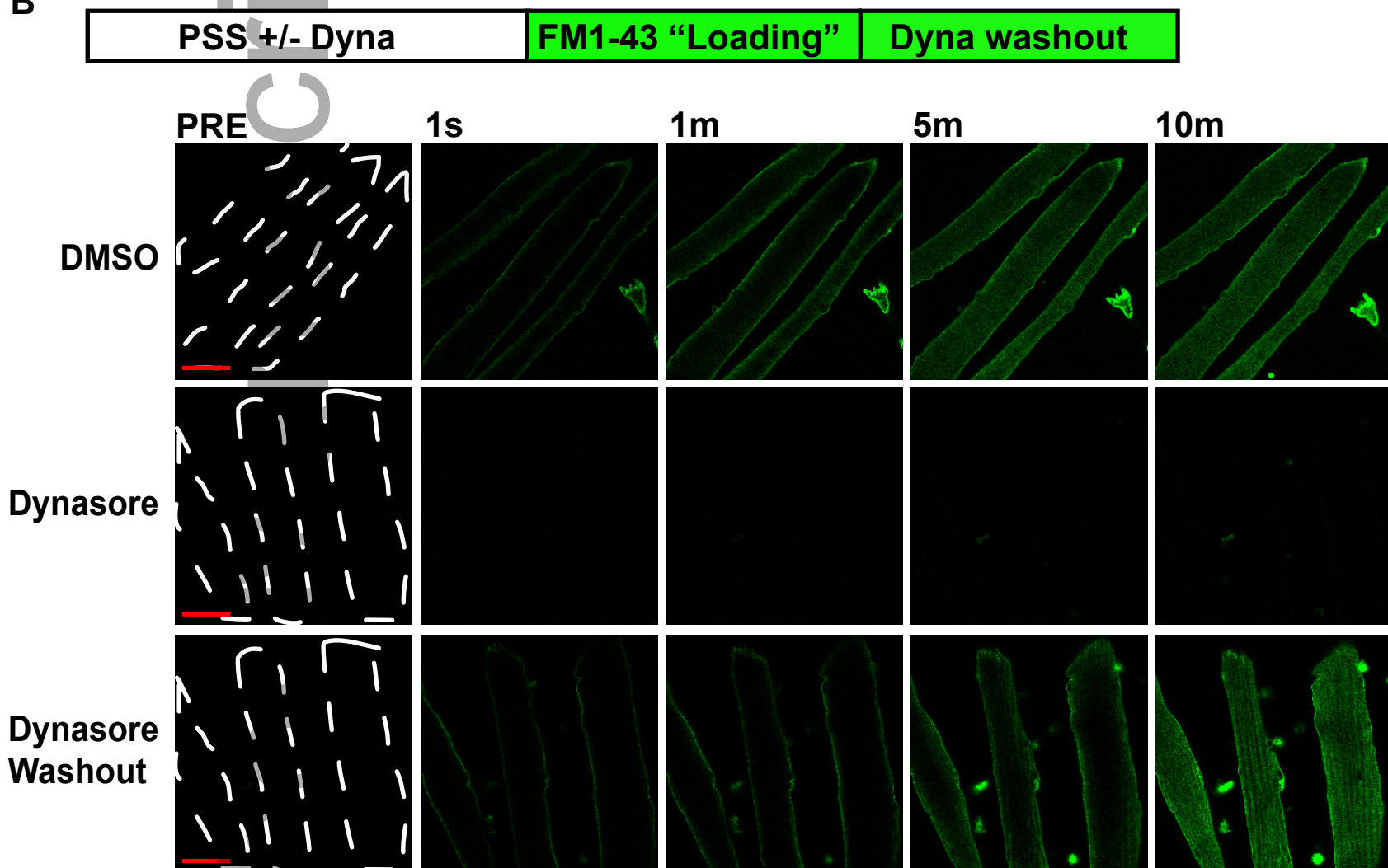
647
648
649
650
651

Author Manuscript

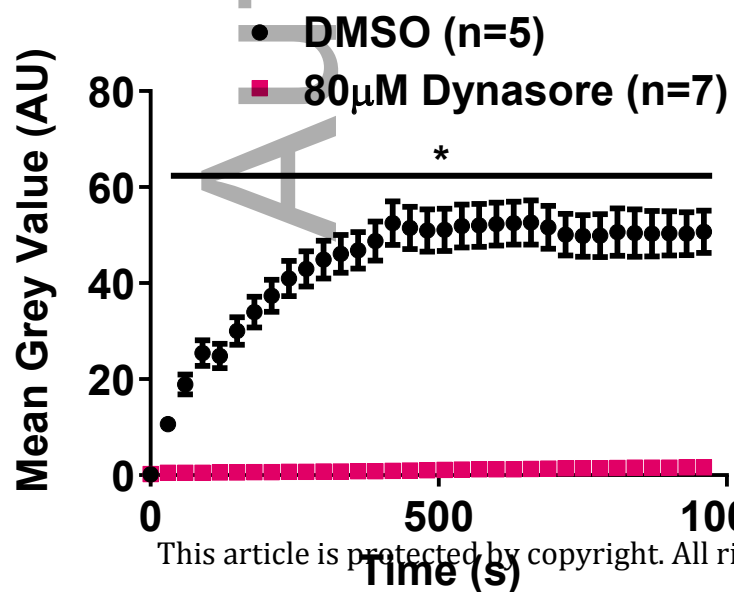
A



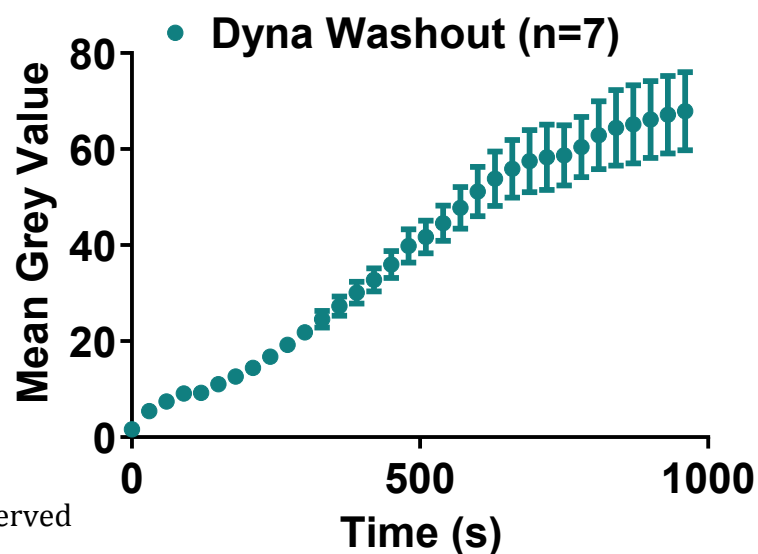
B

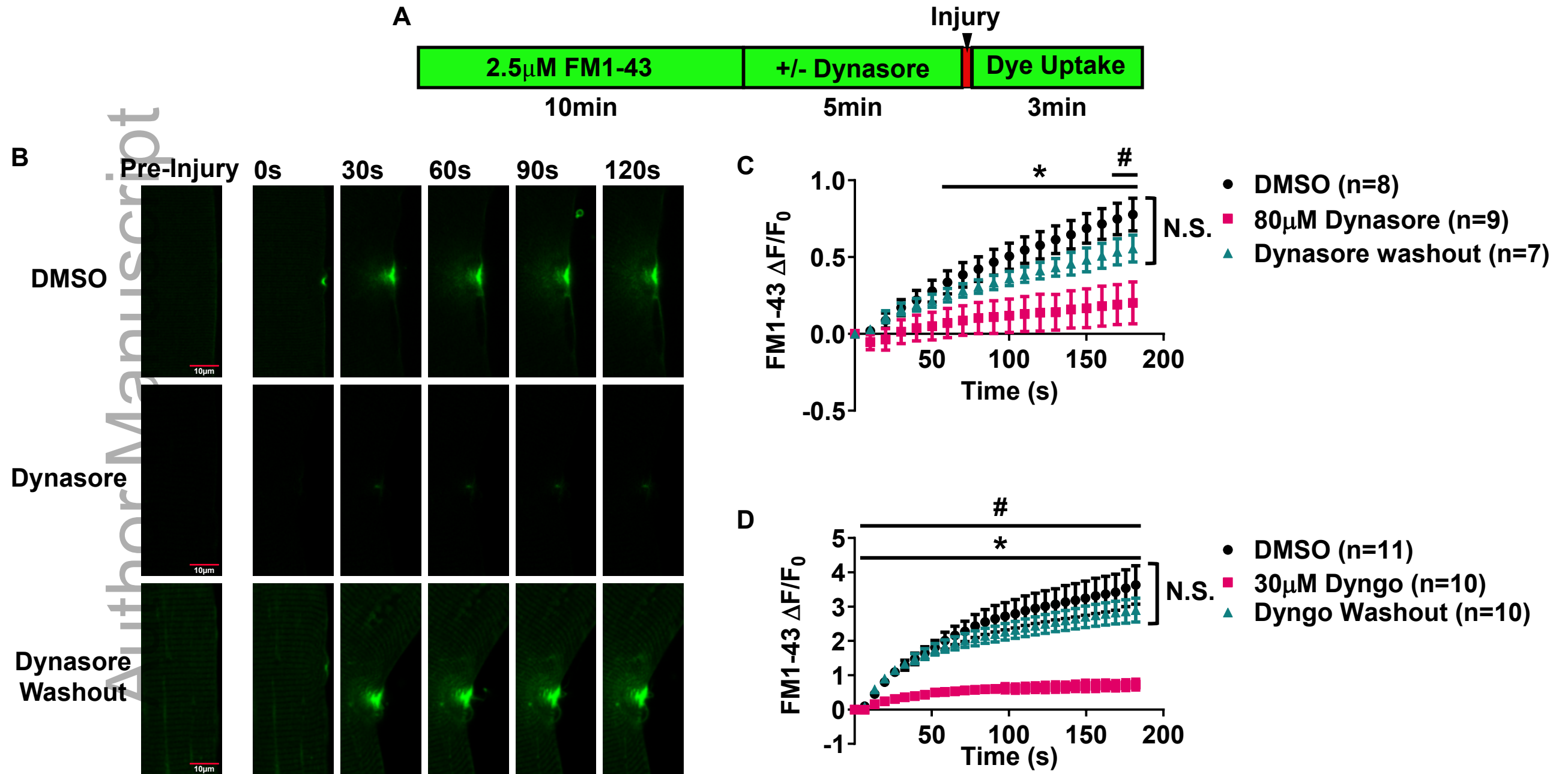


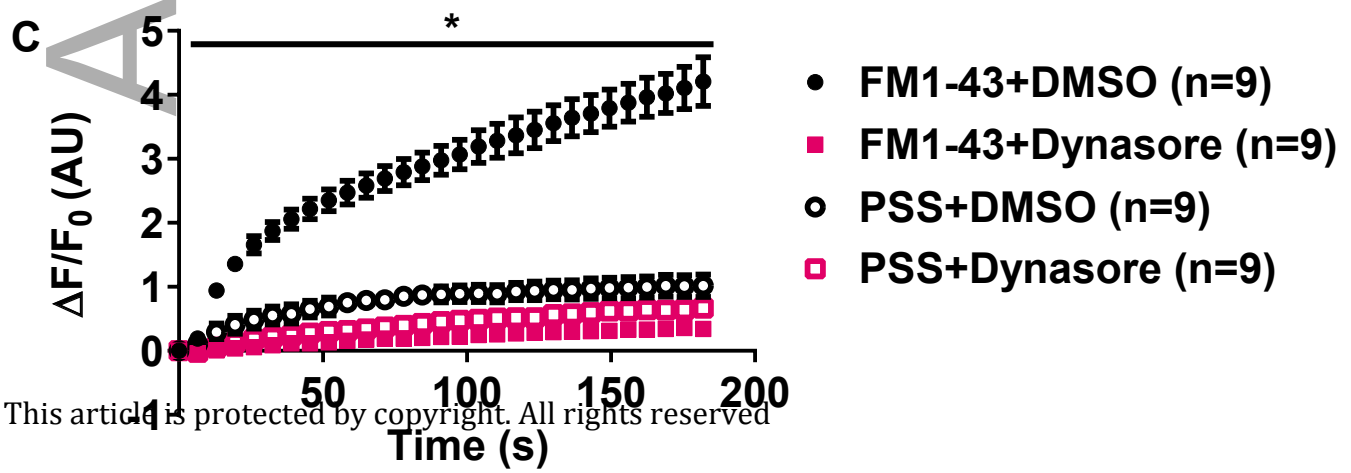
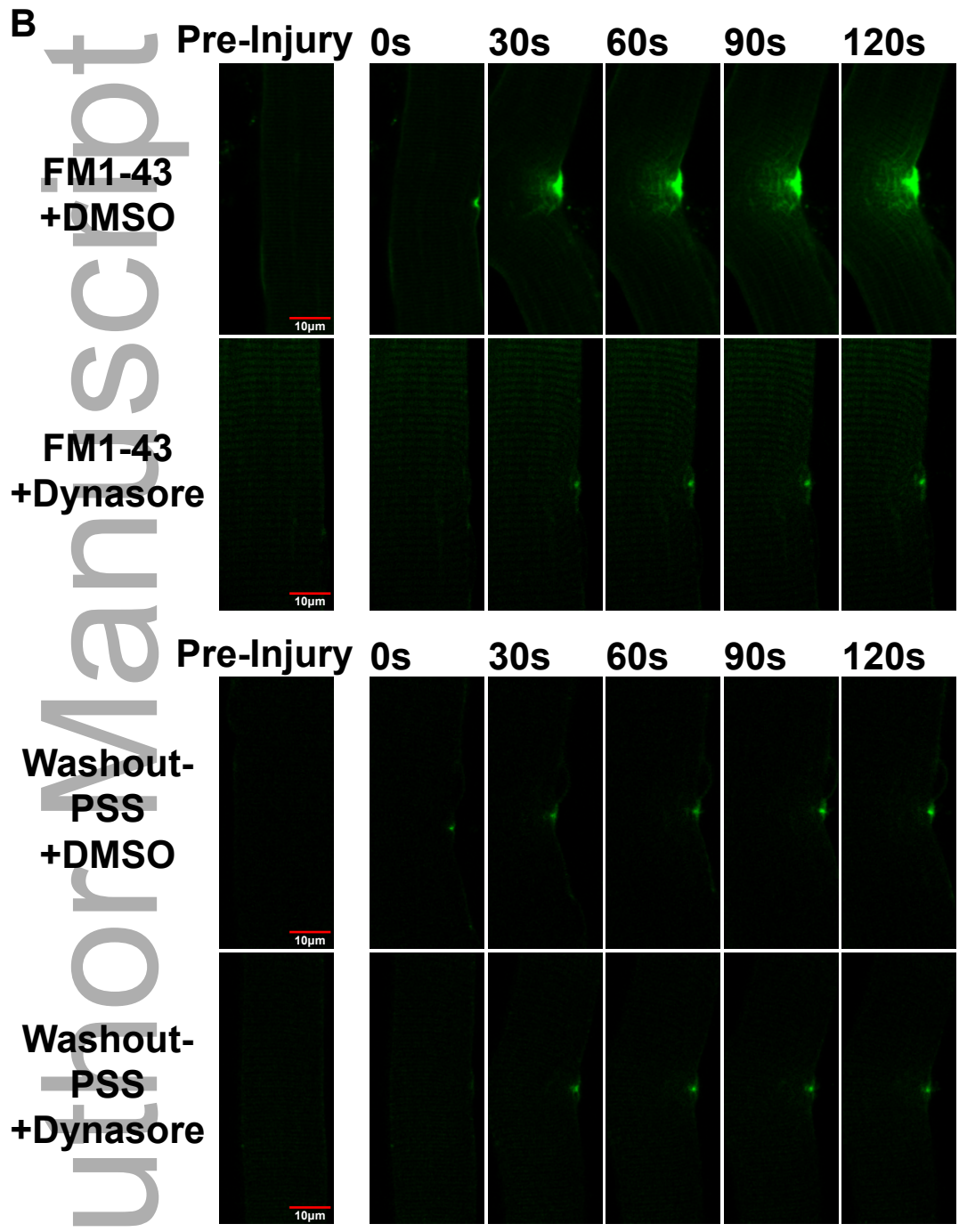
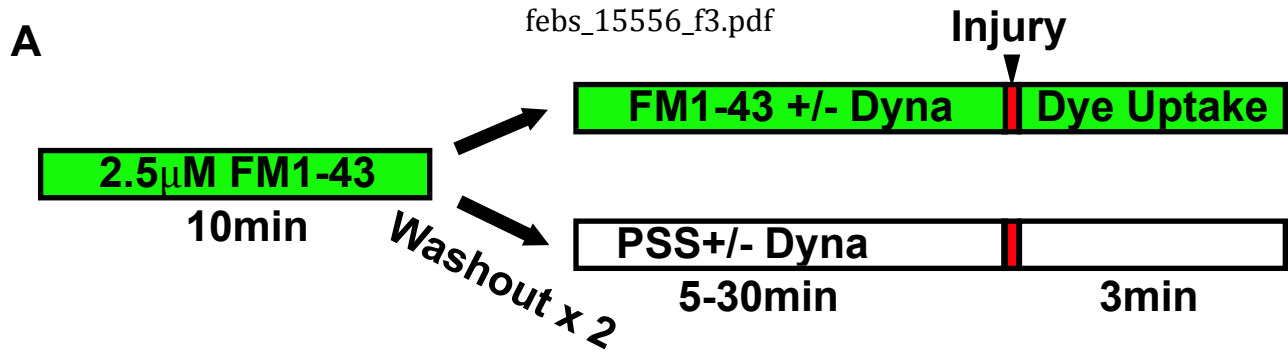
C

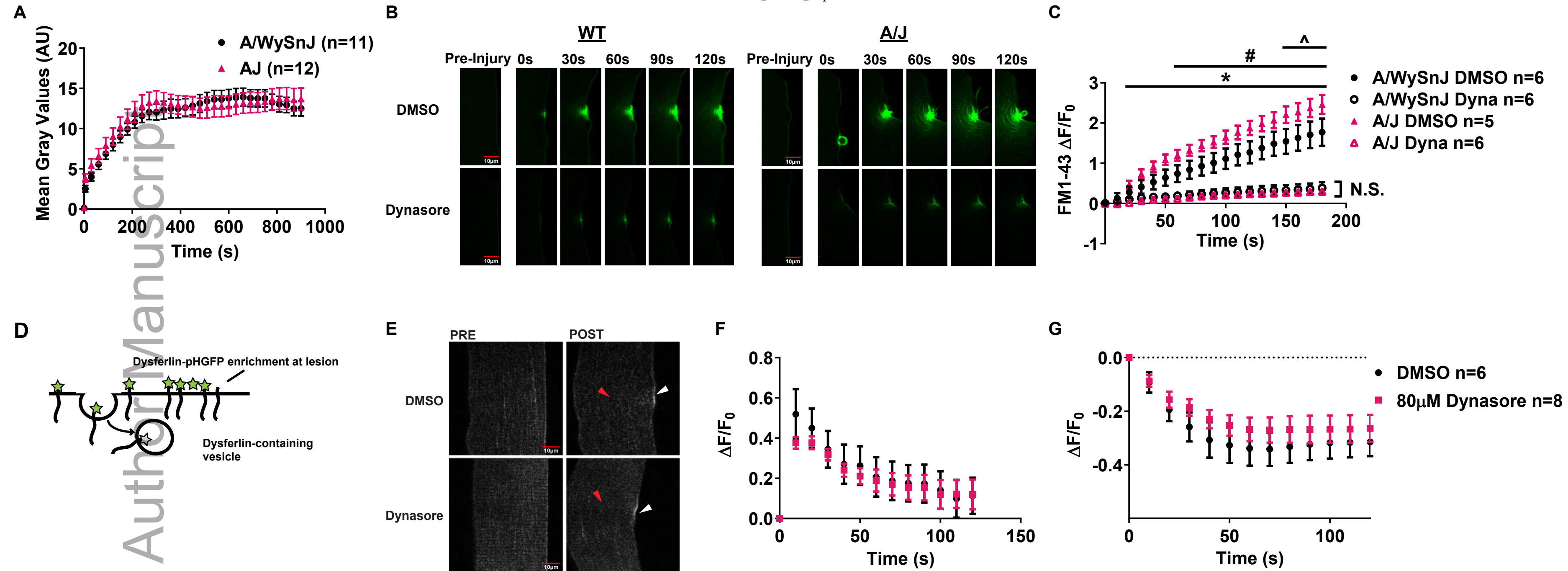


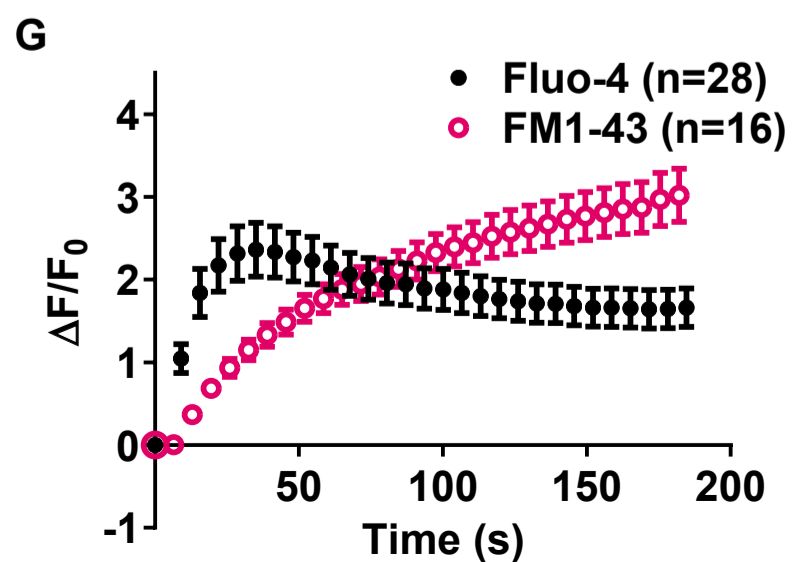
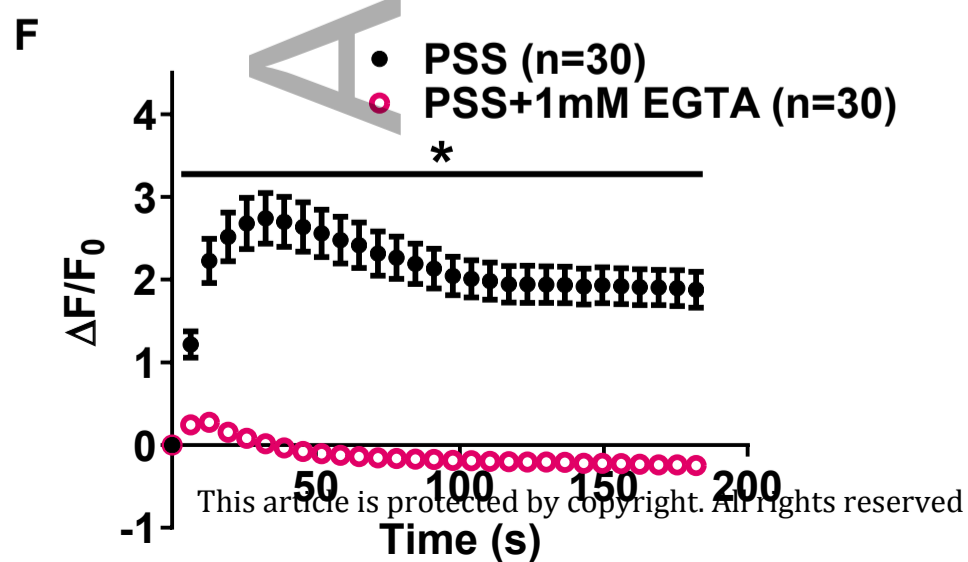
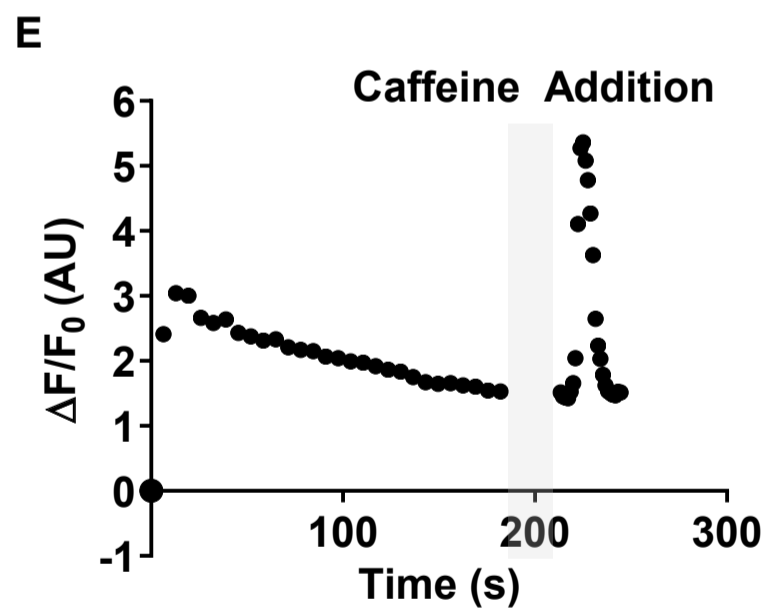
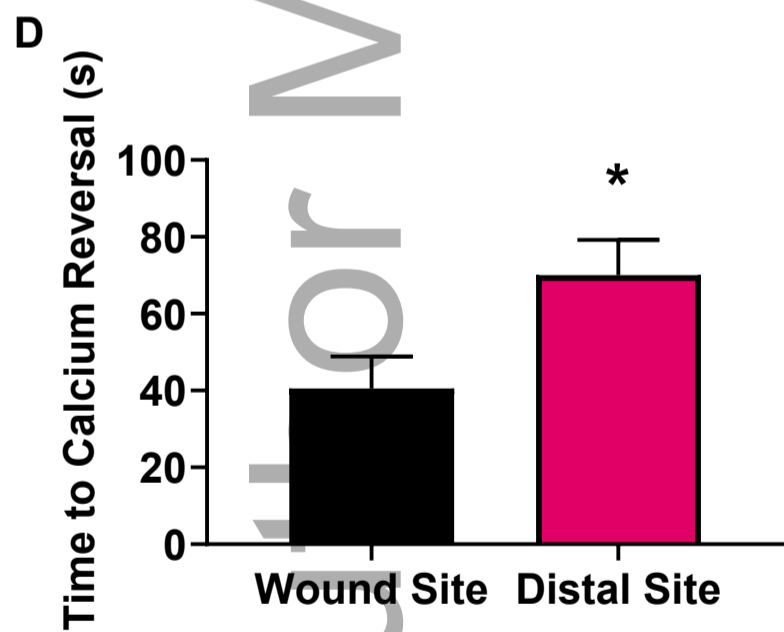
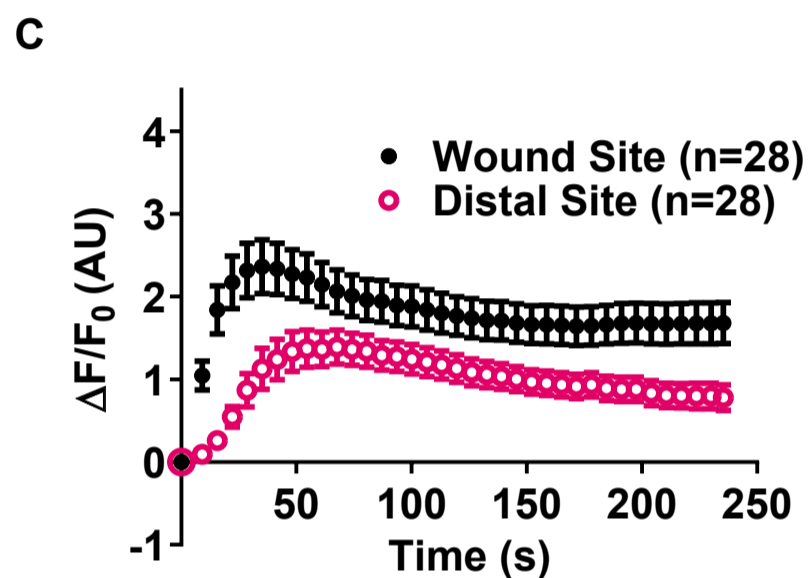
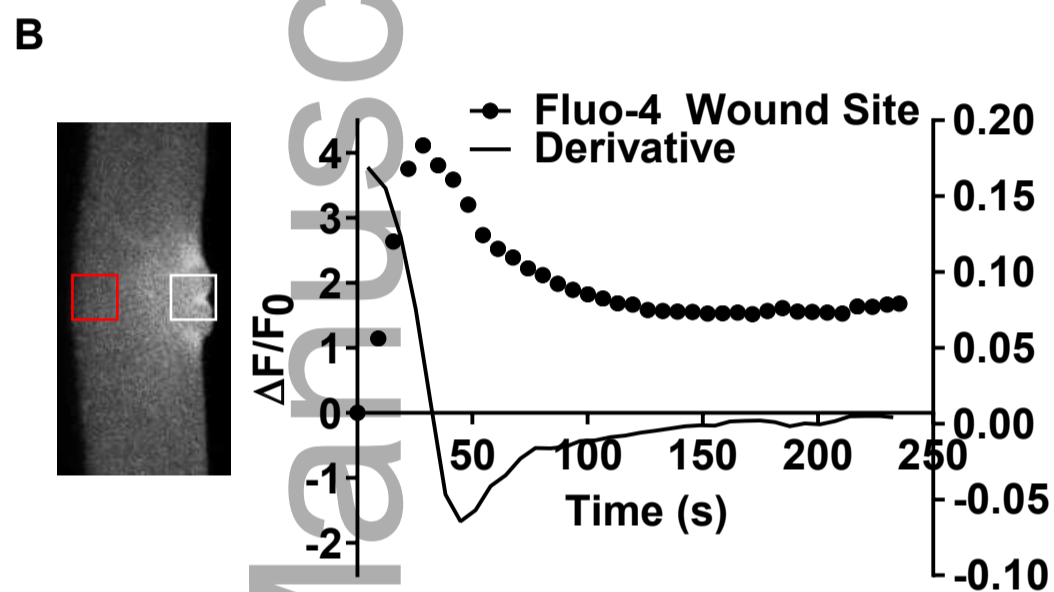
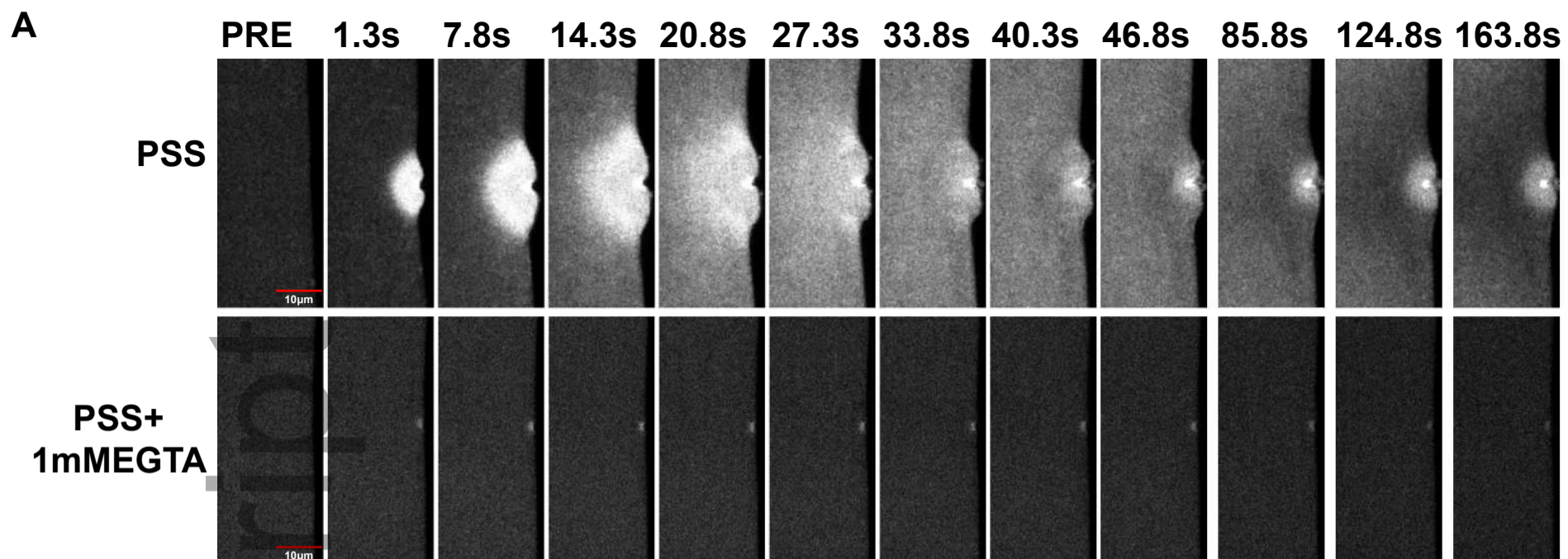
D

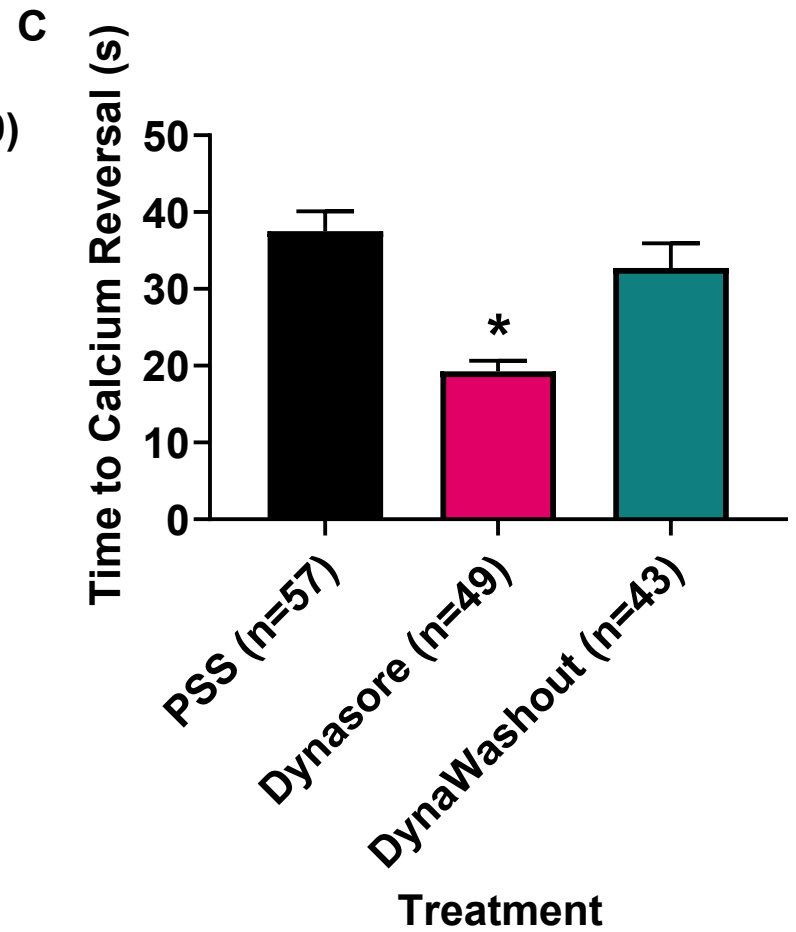
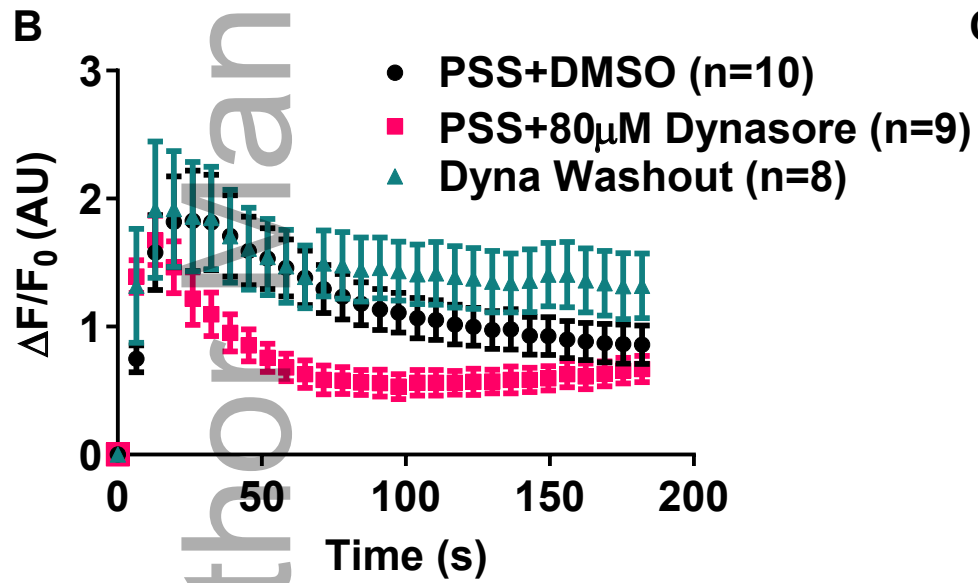
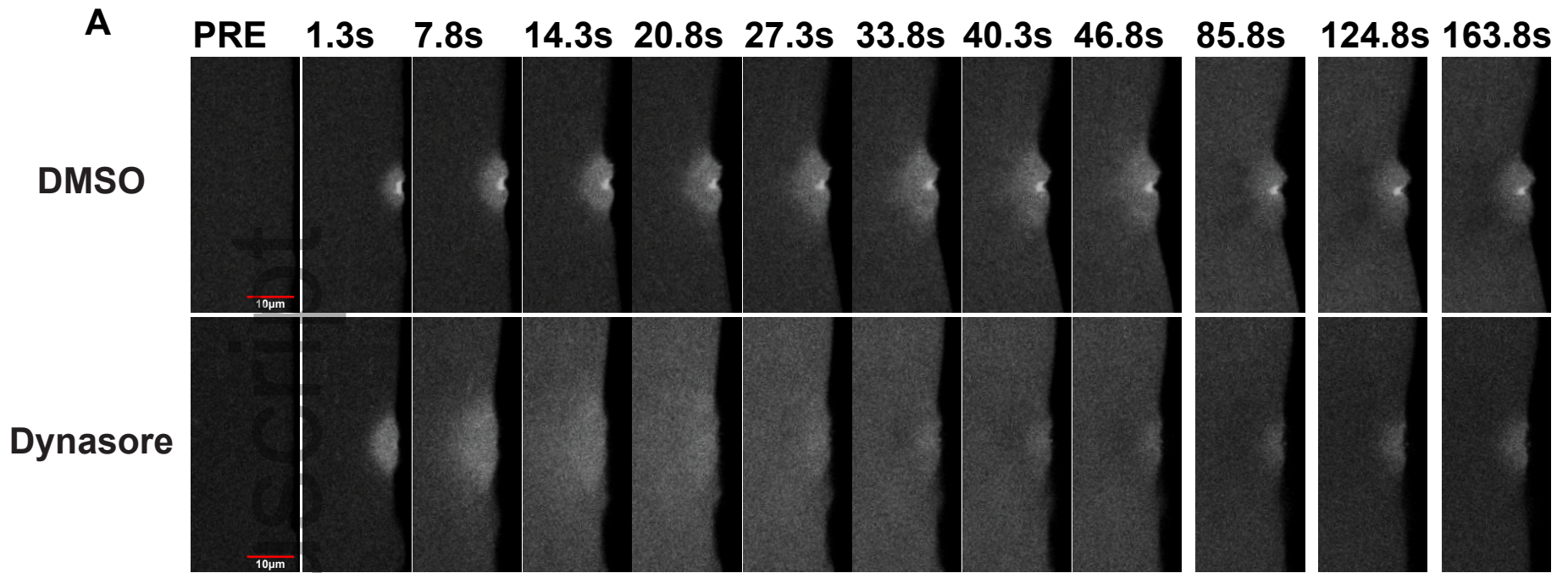




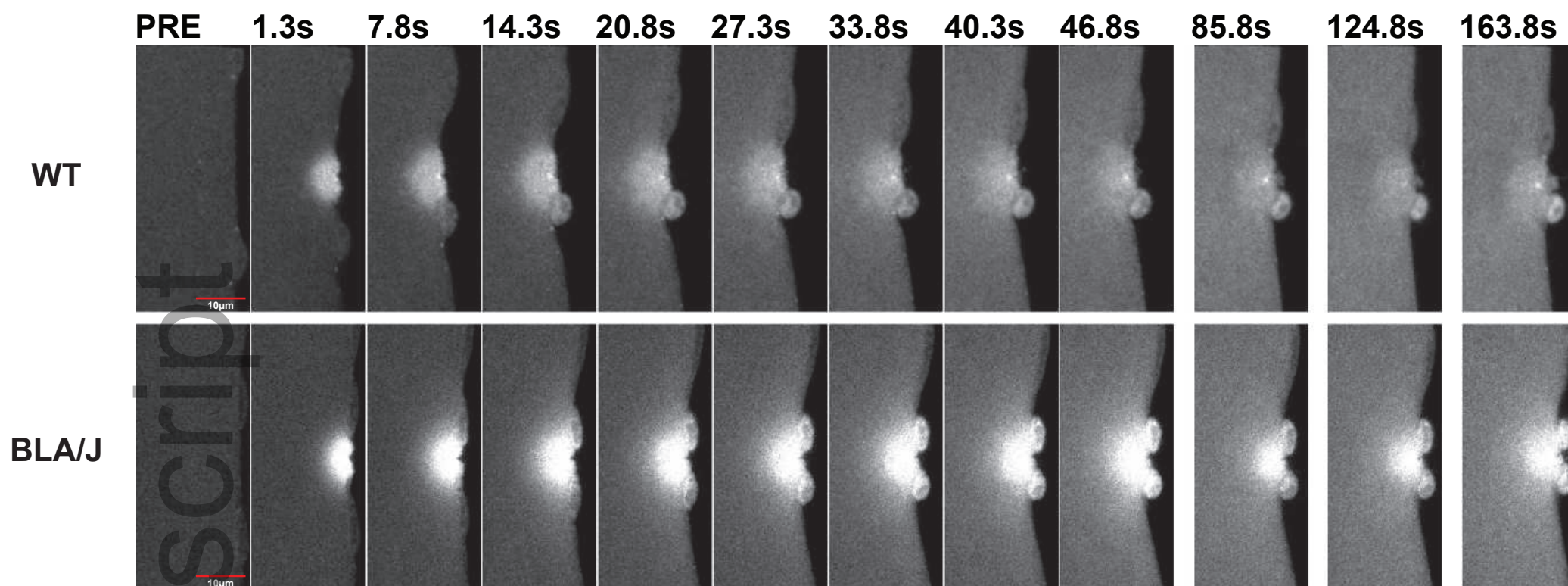




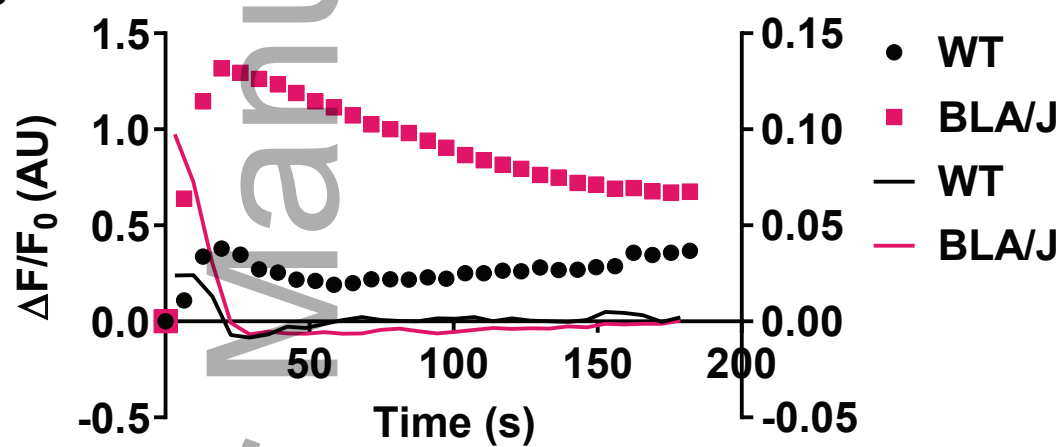




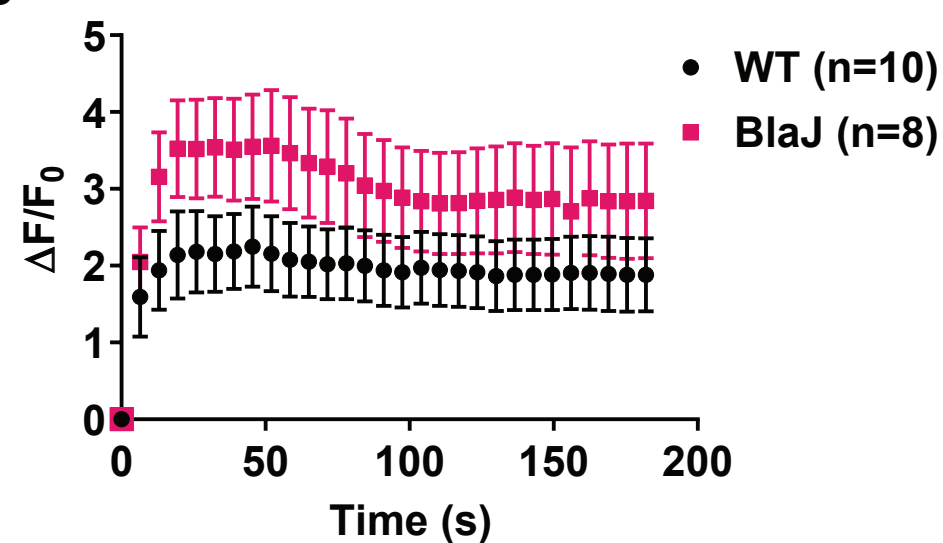
A



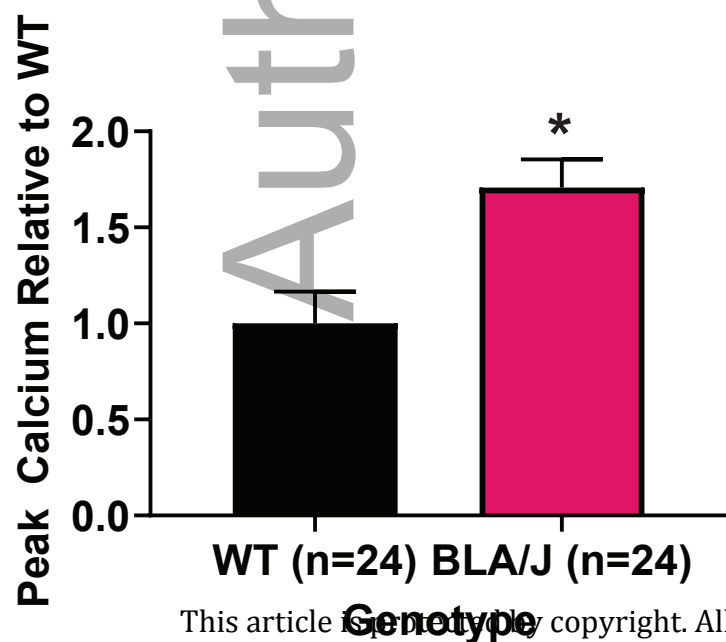
B



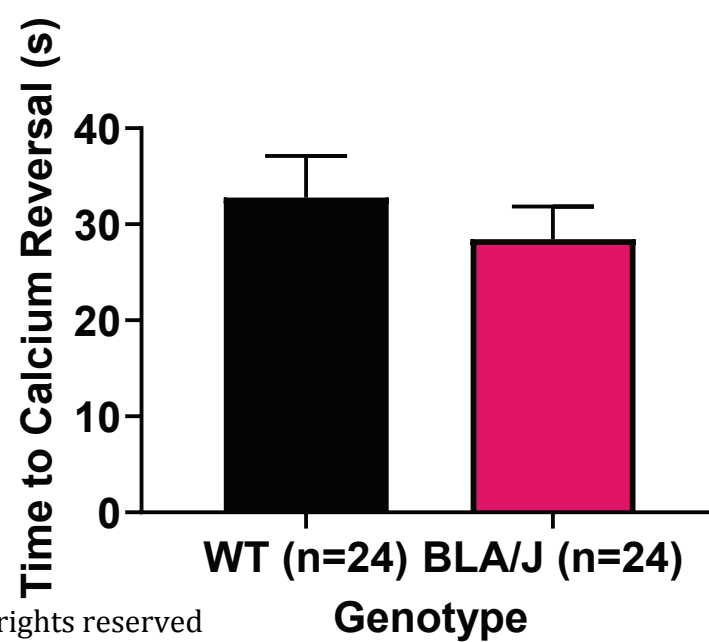
C



D



E



F

